

The modular S -matrix as order parameter for topological phase transitions

F A Bais^{1,2} and J C Romers¹

¹ Institute for Theoretical Physics, University of Amsterdam, Science Park 904, P.O.Box 94485, 1090 GL Amsterdam, The Netherlands

E-mail: j.c.romers@uva.nl

² Santa Fe Institute, Santa Fe, NM 87501, USA

Abstract. We study topological phase transitions in discrete gauge theories in two spatial dimensions induced by the formation of a Bose condensate. We analyse a general class of euclidean lattice actions for these theories which contain one coupling constant for each conjugacy class of the gauge group. To probe the phase structure we use a complete set of open and closed anyonic string operators. The open strings allow one to determine the particle content of the condensate, whereas the closed strings enable us to determine the matrix elements of the modular S -matrix, also in the broken phase. From the measured broken S -matrix we may read off the sectors that split or get identified in the broken phase, as well as the sectors that are confined. In this sense the modular S -matrix can be employed as a matrix valued non-local order parameter from which the low-energy effective theories that occur in different regions of parameter space can be fully determined.

To verify our predictions we studied a non-abelian anyon model based on the quaternion group $H = \bar{D}_2$ of order eight by Monte Carlo simulation. We probe part of the phase diagram for the pure gauge theory and find a variety of phases with magnetic condensates leading to various forms of (partial) confinement in complete agreement with the algebraic breaking analysis. Also the order of various transitions is established.

PACS numbers: 73.43.-f, 71.10.Pm

1. Topological order and topological symmetry breaking

1.1. Introduction

In recent years there has been a growing interest in systems that allow for the realisation of different topological phases, the examples can be found in Levin-Wen models [1], the Kitaev Honeycomb model [2], discrete gauge theories [3], and last but not least in quantum Hall systems [4, 5, 6, 7, 8]. Many of these can be understood from the point of view of topological symmetry breaking where a Bose condensate forms [3, 9]. This breaking is very similar to ordinary symmetry breaking but it uses nonlocal order parameters carrying anyonic quantum numbers. In most of the examples quoted a Hamiltonian framework is used, but in this paper we show that to analyse such systems it could be profitable to switch to a euclidean action formulation which allows for the use of Monte Carlo simulations to determine the phase structure, and more specifically makes it possible to directly obtain the modular S -matrix of the broken phases. After briefly recalling the basic ingredients of topological order and topological symmetry breaking and settle some notation, we show how open string operators and the modular S -matrix can be used as order parameters and phase indicators for topological symmetry breaking. We then introduce a class of lattice actions for discrete gauge theories and verify the theoretical analysis in detail by numerical simulations.

1.2. TQFT basics

In this section we set the stage and fix the notation for the rest of this paper. We study phases of systems that are described by a Topological Quantum Field Theory (TQFT) in $2 + 1$ dimensions. We label the different sectors or (anyonic) particle species by a, b, c, \dots . The two interactions between two particles in a TQFT are fusion and braiding.

Fusion We describe fusion by the rule

$$a \times b = \sum_c N_c^{ab} c, \quad (1)$$

where the integer multiplicities N_c^{ab} give the number of times c appears in the fusion product of a and b . The fusion algebra is associative and commutative, and has a unique identity element denoted as “1” that represents the vacuum. Each sector a has a unique conjugate \bar{a} (representing the corresponding anti anyon) with the property that their fusion product contains the identity:

$$a \times \bar{a} = 1 + \sum_{c \neq 1} N_c^{a\bar{a}} c.$$

Braiding The particles in a $2 + 1$ dimensional TQFT can have fractional spin and statistics. Rotating a particle a by 2π (also called *twisting*) multiplies the state vector

by a phase equal to the *spin factor* θ_a

$$|a\rangle \xrightarrow{\text{twist}} \theta_a |a\rangle,$$

generalizing the usual $+1$ (-1) known from bosons (fermions) in $3 + 1$ dimensions. Adiabatically moving a particle a around another particle b in a channel c is called a *braiding* and can have a nontrivial effect on the state vector of the system, given by $\theta_c/\theta_a\theta_b$.

Quantum dimensions The quantum dimensions d_a of particle species a are another set of important quantities in a TQFT. These numbers satisfy the fusion rules (1), i.e. $d_a d_b = \sum_c N_c^{ab} d_c$. The quantum dimension of an anyonic species is a measure for the effective number of degrees of freedom, corresponding to the internal Hilbert space of the corresponding particle type. The Hilbert space dimension of a system with N identical particles of type a grows as $(d_a)^N$ for N large. In general, the quantum dimensions d_a will be real numbers; however for DGTs they are integers. The total quantum dimension \mathcal{D} of the theory is given by

$$\mathcal{D} = \sqrt{\sum_i d_i^2},$$

and the topological entanglement entropy of the ground state is proportional to $\log \mathcal{D}$.

Diagrammatics There is a powerful diagrammatic language to express the equations describing the TQFT, which we will use to relate the values of observables as they can be measured in the different phases. In this paper we will use the notation and definitions given by Bonderson in [10]. Particle species are represented by lines, fusion and splitting by vertices. A twist is represented by a left or right twist on a particle line:

$$\begin{array}{c} \uparrow \\ \circlearrowleft \\ a \end{array} = \theta_a \begin{array}{c} \uparrow \\ | \\ a \end{array}, \quad \begin{array}{c} \circlearrowright \\ a \end{array} = \theta_a^* \begin{array}{c} \uparrow \\ | \\ a \end{array}. \quad (2)$$

The evaluation of simple diagrams is rather straightforward, and complicated diagrams can be simplified using braid relations and the so-called F symbols which follow from associativity of the fusion algebra. The simplest examples are the closed loop of type a that evaluates to the quantum dimension d_a :

$$a \circlearrowleft = d_a, \quad (3)$$

whereas the twisted loop equals $d_a \theta_a$:

$$\begin{array}{c} \circlearrowleft \\ \circlearrowright \\ a \end{array} = \theta_a d_a \quad (4)$$

Of particular interest are the generators of the modular group, S_{ab}

$$\begin{array}{c} \circlearrowleft \\ \circlearrowright \\ a \quad b \end{array} = S_{ab} = \frac{1}{\mathcal{D}} \sum_c N_c^{a\bar{b}} \frac{\theta_c}{\theta_a \theta_b} d_c, \quad (5)$$

and $T_{ab} = e^{-2\pi i(\bar{c}/24)}\theta_a\delta_{a,b}$. As we mentioned before the importance of the rather abstract diagrammatic notation is that the diagrams directly correspond to observables in our euclidean lattice gauge theory formulation. In the euclidean three dimensional formulation of topological theories the values these diagrams have, correspond to the vacuum expectation values of the corresponding anyon loop operators, for example in the unbroken phase one may measure

$$\left\langle a \circlearrowleft \right\rangle_0 = d_a, \quad (6)$$

where the l.h.s. is now defined as the value of the path integral with the nonlocal loop operator for particle species a inserted and the r.h.s. is obtained if we are probing the system in the unbroken phase governed with the groundstate denoted as 0 and governed by the algebra \mathcal{A} . We use the subscript 0 because the value of the same diagram may be different if it is evaluated in a different phase with a groundstate that we will denote by Φ ; in the remainder of the paper we will therefore always use brackets with a subscript.

1.3. Topological symmetry breaking

In this section we briefly recall topological symmetry breaking, the phenomenon that a phase transition to another topological phase occurs due to a Bose condensate [3]. The analogy with ordinary symmetry breaking is clear if one thinks of the particle as representations of some quantum group, and assumes that a bosonic degree of freedom i.e. with $\theta_c = 1$ – fundamental or composite – condenses. The breaking can then be analyzed, either from the quantum group (Hopf algebra) point of view, or from the representation theory point of view. In the case of general quantum groups it is the latter approach which is the most natural and powerful in the context of TQFT because the fusion algebra corresponds to the representation ring of the quantum group. A general treatment with ample examples can be found in reference [9]. The breaking procedure involves two steps, firstly the condensate reduces the unbroken fusion algebra (also called a braided modular tensor category) \mathcal{A} to an intermediate algebra denoted by \mathcal{T} . This algebra however may contain representations that braid nontrivially with the condensed state, i.e. with the new vacuum and if that is the case, these representation will be confined and will be expelled from the bulk to the boundary of the sample. Confinement implies that in the bulk only the unconfined sectors survive as particles and these are characterized by some subalgebra $\mathcal{U} \subset \mathcal{T}$. We briefly describe the two steps separately.

From \mathcal{A} to \mathcal{T} Assuming that a certain bosonic irrep c will condense due to some underlying interaction in the system, implies that c will be identified with the vacuum of \mathcal{T} . For our purposes, a boson is a sector with trivial (integer) spin, though in fact in the context of 2 + 1 dimensions one has to also require that fusion of this field with itself has a channel with trivial braiding.

The definition of the new vacuum requires to a redefinition of fields. Firstly, fields in \mathcal{A} that appear in the orbit under fusion with the condensed field c are identified in

\mathcal{T} , so, if $c \times a = b$ then $a, b \rightarrow a'$. Secondly, if a field b forms a fixed point under fusion with the condensate c , then the field will split at least in two parts: $b \rightarrow \sum_i b_i$. The identifications and splittings of representations can be summarized by a rectangular matrix n_a^t that specifies the “branching” or “restriction” of fields a from in \mathcal{A} to \mathcal{T} with fields t, r, s, \dots :

$$a \rightarrow \sum_t n_a^t t$$

This *branching matrix* is a rectangular matrix (the number of particle types in the \mathcal{A} and \mathcal{T} theories is not equal in general) of positive integers. We will also consider the transpose of this matrix denoted as n_t^a which specifies the “lift” of the fields $t \in \mathcal{T}$ to fields $a \in \mathcal{A}$:

$$t \rightarrow \sum_a n_t^a a = \sum_{a \in t} a$$

One may now derive the fusion rules \mathcal{T} from the fusion algebra (1). Because of the identifications, it is often the case that the intermediate algebra \mathcal{T} though being a consistent fusion algebra, is not necessarily braided, in more technical terms, it satisfies the “pentagon” equation but not the “hexagon” equation. The physical interpretation of this fact is that the sectors in \mathcal{T} do not yet constitute the low energy effective theory, this is so because the sectors that have an ambiguous spin factor will be connected to a domain wall and hence are confined in the new vacuum. The confined excitations will be expelled to the edges of the system or have to form hadronic composites that are not confined. Yet the \mathcal{T} algebra plays an important role: in [6] for example, it was shown that the \mathcal{T} algebra governs the edge/interface degrees of freedom in the broken phase.

From \mathcal{T} to \mathcal{U} Some of the sectors in \mathcal{T} will survive in the bulk, some will be confined. The physical mechanism behind confinement in $2 + 1$ dimensional topological field theories is nontrivial braiding with the condensate. The vacuum state or order parameter should be single valued if carried adiabatically around a localized particlelike excitation. If it is not single valued that would lead to a physical string or “domain wall” extending from the particle that carries a constant energy per unit length. The unconfined algebra \mathcal{U} consists of the representations in \mathcal{T} minus the confined ones, it is this algebra that governs the low energy effective bulk theory. The confined representations can be determined in the following way. First we define the “lift” of a representation in \mathcal{T} as the set of representations $b \in \mathcal{A}$ that restrict to t . Now, if all of the representations in the lift of t braid trivially with the lift of the vacuum, the sector t is part of \mathcal{U} . Otherwise, it is confined. One may prove that the \mathcal{U} algebra closes on itself with consistent fusion rules, while consistent braiding is achieved by assigning the (identical) spin factors of the parent sectors of the unbroken theory to the \mathcal{U} fields.

Let us finally mention the so-called *quantum embedding index* q defined in [11], it is a real number characterizing the topological symmetry breaking. This quantity is

defined as

$$q = \frac{\sum_a n_u^a d_a}{d_u}, \quad (7)$$

where the index a runs over the sectors of the unbroken phase \mathcal{A} , that correspond to lift of any sector u or t of the algebra \mathcal{U} or \mathcal{T} ; the n_u^a is the lift of sectors u to their parents a and d_a is the quantum dimension of the representation a . Observe that this expression is independent of the particular sector u . Choosing for u the new vacuum, we obtain that q just equals the total quantum dimension of the lift of the \mathcal{U} (or \mathcal{T}) vacuum in the unbroken \mathcal{A} theory. As an aside we mention that the change in topological entanglement entropy of the disk changes also by $\log(\mathcal{D}_{\mathcal{A}}/\mathcal{D}_{\mathcal{U}}) = \log q$ in a transition from an \mathcal{A} to a \mathcal{U} phase [11].

1.4. Observables

Our objective is to verify the theoretical predictions of the topological symmetry breaking scheme in a class of euclidean gauge theories that are expected to exhibit transitions between different topological phases. We will numerically evaluate the expectation values of various topological diagrams using Monte Carlo simulations, and in this section we calculate the predicted outcomes of a variety of possible measurements from theory. The strategy has two steps, (i) the determination of the condensate (including the measurement of the embedding index q) by evaluating the basic nonlocal open string order parameters, (ii) measuring the so-called broken modular S -matrix and from that construct the S -matrix of the \mathcal{U} phase. We also will see that the condensate fixes the branching and lift matrices and having determined those we can also predict the outcome of measurements of other topological diagrams corresponding to the lifts of \mathcal{U} fields to \mathcal{A} fields .

1.4.1. Determination of the condensate and the embedding index q . We measure the open string operators in the model. If the symmetry is unbroken we will have for any nontrivial field a that

$$\langle L_{a\bar{a}} \rangle_0 = \left\langle \left| \begin{array}{c} \uparrow \\ a \end{array} \right\rangle_{\Phi=0} \right\rangle = 0. \quad (8)$$

because the diagram represents the creation and subsequent annihilation of a single a -particle. However in the broken situation the expectation value will be nonzero for all fields $\phi_i \in \mathcal{A}$ in the condensate which we denote by Φ . So writing,

$$\Phi = 0 + \sum_i \phi_i \quad (9)$$

we obtain that in general,

$$\left\langle \left| \begin{array}{c} \uparrow \\ a \end{array} \right\rangle_{\Phi} \right\rangle = \delta_{a\phi_i} d_a. \quad (10)$$

This in turn implies that it is simple to measure q as

$$\sum_{a \in \mathcal{A}} \left\langle \left| \begin{array}{c} \uparrow \\ a \end{array} \right\rangle_{\Phi} \right\rangle = \left\langle \left| \begin{array}{c} \uparrow \\ 0 \end{array} \right\rangle_{\Phi} \right\rangle + \sum_i \left\langle \left| \begin{array}{c} \uparrow \\ \phi_i \end{array} \right\rangle_{\Phi} \right\rangle = d_0 + \sum_i d_{\phi_i} = q \quad (11)$$

1.4.2. Determination of confinement and other topological data of the broken phase. Once we have determined the components of the vacuum we can determine the lifts of the t fields simply by studying the fusion rules of $\Phi \times a = \sum t'$, where t' denotes the lifts of those t fields which contain a , i.e. for which $n_t^a = 1$. Having obtained the lifts of the t fields the next step is to make the measurement determining whether a given t field is confined. This involves the measurement of the index η , or simply:

$$\left\langle \sum_{a \in t} \left(\bigcirc \right)_a \right\rangle_{\Phi} = q \sum_{a \in t} \theta_a d_a = q^2 d_t \eta_t = \begin{cases} 0 & \text{if } t \notin \mathcal{U} \text{ (confined)} \\ q^2 \theta_u d_u & \text{if } t \in \mathcal{U} \text{ (not confined)} \end{cases} \quad (12)$$

Alternatively one can measure certain closed a_i loop operators that are also defined for fields a that split under branching and that will be defined later, for which holds that:

$$\left\langle \left(\bigcirc \right)_{a_i} \right\rangle_{\Phi} = \left\langle \left(\bigcirc \right)_{a_i} \right\rangle_0 + \sum_j \left\langle \left(\bigcirc \right)_{a_i \phi_j} \right\rangle_0 = \begin{cases} 0 & \text{if } t \notin \mathcal{U} \text{ (confined)} \\ q^2 \theta_u d_u & \text{if } t \in \mathcal{U} \text{ (not confined)} \end{cases} \quad (13)$$

It follows that from these measurements, the fields that are confined can be determined, but also the quantum dimensions d_u and twists θ_u of the unbroken \mathcal{U} theory are obtained.

1.4.3. The broken modular S - and T -matrices. Instead of the fusion coefficients N_c^{ab} an alternative specification of a (modular) topological field theory is by its representation of the modular group $SL(2, \mathbb{Z})$ generated by the S and T -matrices

$$S^2 = (ST)^3 = \mathcal{C}, \quad S^* = \mathcal{C}S = S^{-1}, \quad T^* = T^{-1}, \quad \mathcal{C}^2 = 1, \quad (14)$$

with \mathcal{C} the charge conjugation matrix. The corresponding matrix elements can be expressed in the fusion coefficients and spin factors:

$$S_{ab} = \frac{1}{\mathcal{D}} \sum_c N_c^{a\bar{b}} \frac{\theta_c}{\theta_a \theta_b} d_c, \quad (15)$$

$$T_{ab} = e^{-2\pi i(\bar{c}/24)} \theta_a \delta_{a,b} \quad (16)$$

where \mathcal{D} is the total quantum dimension and the constant \bar{c} is the conformal central charge of the corresponding conformal field theory. We recall that the central charge of a discrete gauge theory is zero, so in that case the T -matrix is just the diagonal matrix containing the spin factors.

The great advantage of switching to the modular data is that unlike the fusion coefficients these generators can be directly measured using the anyon loop operators that arise naturally in a three dimensional euclidean formulation of the theory. We will evaluate the expectation value of these S -matrices numerically in our lattice formulation

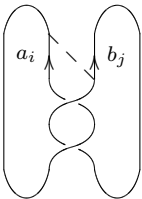
of multiparameter discrete gauge theories later on. The measured S - and T -matrix elements do not satisfy the relations (14) directly; however, using the measurements the full S - and T -matrices of the \mathcal{U} theory, which do satisfy the modular group relations, can be constructed. In the unbroken theory the measured S -matrix elements $\langle S_{ab} \rangle$ correspond to the expectation values of the Hopf link with one loop colored with representation a and the other with representation b :

$$\langle S_{ab} \rangle_0 = \frac{1}{\mathcal{D}} \left\langle a \left(\bigcirc \bigcirc \right)_b \right\rangle_0 = S_{ab},$$

where S_{ab} is the S -matrix of the unbroken \mathcal{A} theory. We can however also determine the modular S -matrix of the residual \mathcal{U} theory directly from measurements if we take the splittings of certain fields $a \Rightarrow \{a_i\}$ in account appropriately. We will show how to do this later for the DGT's in detail and give a more general mathematical treatment of this elsewhere [12]. Then we will arrive at an explicit formula and algorithm to determine S_{uv} :

$$S_{uv} = \frac{1}{q} \sum_{a_i, b_j} n_u^{a_i} n_v^{b_j} \langle S_{a_i b_j} \rangle_{\Phi}. \quad (17)$$

This expression involves not only the branching (lift) matrix $n_u^{a_i}$, but also the what we will call the *broken S -matrix* defined as $\tilde{S}_{a_i b_j} = \langle S_{a_i b_j} \rangle_{\Phi}$, which, because of the splitting, clearly involves a larger size matrix than the modular S -matrix of the original \mathcal{A} phase. From the broken S -matrix we may directly read off S_{uv} , the S -matrix of the effective low energy TQFT governed by \mathcal{U} . An important observation is that the values of the S -matrix elements in a broken phase will be different from the ones in the unbroken phase, for example because of the contribution of the *vacuum exchange diagram* \tilde{S} depicted below, in which the condensed particle is exchanged giving a nonzero contribution in the broken phase while it would give a vanishing contribution in the unbroken phase:

$$\tilde{S}_{a_i b_j} = \frac{1}{q^2} \left(\text{diagram} \right)$$


In the explicit calculations later on we show that this *vacuum exchange diagram* leads to a change in the S -matrix which depends on the subindices introduced above. It turns out that it is also possible to calculate the broken S -matrix from first principles, this will be discussed in a forthcoming paper [12].

As to be expected one finds identical rows and columns in the broken S -matrix, for components that are identified, whereas the entries for confined fields will be zero. With this prescription the formalism outlined above is applicable in any phase of the theory including the unbroken one where there is no splitting and the vacuum exchange diagram gives a vanishing contribution. The measured T -matrix on the other hand is

given by

$$\langle T_{ab} \rangle_{\Phi} = \frac{\delta_{ab}}{d_a} \left\langle \left(\bigcirc \right)_a \right\rangle_{\Phi}$$

again with $\langle T_{ab} \rangle_0 = T_{ab}$. After measuring or calculating the S - and T -matrices in a given phase, we can reconstruct the fusion coefficients with the help of the Verlinde formula [13],

$$N_{ab}^c = \sum_x \frac{S_{ax} S_{bx} S_{\bar{c}x}}{S_{1x}}. \quad (18)$$

To conclude, we have in this section summarized the basic features of a TQFT and considered some aspects of topological phase transitions induced by a Bose condensate, furthermore we explained how the measurement of the L -, S -, and T -operators in the broken phase fully determine the quantum group of a (broken) topological phase. The general scheme to analyse the breaking pattern of a some multiparameter TQFT is to first use the open string operators to probe which fields are condensed in the various regions of parameter space. In a given broken phase we can subsequently compute/measure what we will call the broken S -matrix $\bar{S}_{a_i b_j}$, where as mentioned the subindex labels the splitting of the corresponding \mathcal{A} field. From the broken S -matrix we can read off the S -matrix of the \mathcal{U} theory. In the remainder of the paper we will explicitly execute this program for discrete gauge theories.

2. A euclidean lattice approach to Discrete Gauge Theories.

2.1. DGT and the quantum double of a finite group

A particular class of TQFT are the so called Discrete Gauge Theories (DGTs). These arise for example if in a (2+1)-dimensional Yang-Mills-Higgs theory the symmetry is broken by a Higgs condensate to a finite subgroup of the (continuous) gauge group. The particles in the theory, their fusion and braiding properties, spins and so forth are all obtained by working out the representation theory of the underlying quantum group, which is the quantum double of the finite discrete subgroup. We will not give a detailed account on the emergence of quantum group symmetry in DGT, this can be found in the literature [14], but do present a short summary of the basics to fix the notation and introduce some key concepts required later on.

Consider the following operators acting on states in the Hilbert space of a DGT. First there is the *flux projection* operator, denoted by P_h , which acts on a state $|\psi\rangle$

$$P_h |\psi\rangle = \begin{cases} |\psi\rangle & \text{if the state } |\psi\rangle \text{ contains flux } h \\ 0 & \text{otherwise} \end{cases}.$$

Secondly, we have the operator g , for each group element $g \in H$, which realizes a global gauge transformation by the element g :

$$g |\psi\rangle = |{}^g \psi\rangle,$$

where it should be noted that we have not yet modded out by the gauge group to obtain the physical Hilbert space. These operators do not commute, and realize the algebra

$$\begin{aligned} P_h P_{h'} &= \delta_{h,h'} P_h \\ g P_h &= P_{ghg^{-1}} g. \end{aligned}$$

The set of combined flux projections and gauge transformations $\{P_h g\}_{h,g \in H}$ generates the quantum double $D(H)$, which is a particular type of algebra called a Hopf algebra.

The representation theory of the quantum double $D(H)$ of a finite group H was first worked out in [15] but here we follow the discussion presented in [16] and follow the conventions of those lecture notes.

Let A be a conjugacy class in H . We will label the elements within A as

$$\{^A h_1, ^A h_2, \dots, ^A h_k\} \in A,$$

for a class A of order k . In general, the centralizers for the different group elements within a conjugacy class are different, but they are isomorphic to one another. Let $^A N \subset H$ be the centralizer for the first group element in the conjugacy class A , denoted by $^A h_1$.

The set $^A X$ relates the different group elements within a conjugacy class to the first:

$$^A X = \{^A x_{h_1}, ^A x_{h_2}, \dots, ^A x_{h_k} \mid ^A h_i = ^A x_{h_i} ^A h_1 ^A x_{h_i}^{-1}\}. \quad (19)$$

This still leaves a lot of freedom, but we fix our convention such that $^A x_{h_1} = e$, the group identity element. The centralizer $^A N$, being a group, will have different irreps, which we label by α . The vector space for a representation α is spanned by a basis $^\alpha v_j$. The internal Hilbert space corresponding to an irrep of the quantum double that combines magnetic and electric degrees of freedom, $V^{(A,\alpha)}$, is then spanned by the set of vectors

$$\{|^A h_i, ^\alpha v_j\rangle\},$$

where i runs over the elements of the conjugacy class, $i = 1, 2, \dots, \dim A$ and j runs over the basis vectors of the carrier space of α , $j = 1, 2, \dots, \dim \alpha$. These irreducible representations correspond precisely to the particle types a, b, \dots in section 1.2. They obey a set of fusion rules as in (1) and it is possible to calculate the modular S -matrix, F -symbols and so on.

To see that this basis is a natural one to act on with our flux measurements and gauge transformations, consider an the matrix action $\Pi^{(A,\alpha)}$ of an irreducible representation (A, α) of some combined projection and gauge transformation $P_h g$:

$$\Pi^{(A,\alpha)}(P_h g) |^A h_i, ^\alpha v_j\rangle = \delta_{h,g ^A h_i g^{-1}} |g ^A h_i g^{-1}, \sum_m D_\alpha(\tilde{g})_{mj} ^\alpha v_m\rangle, \quad (20)$$

where the element \tilde{g} is the part of the gauge transformation g that commutes with the flux $^A h_1$, defined as

$$\tilde{g} = ^A x_{gh_i g^{-1}}^{-1} g ^A x_{h_i}, \quad (21)$$

and $D_\alpha(\cdot)_{ij}$ is the matrix representation of the centralizer.

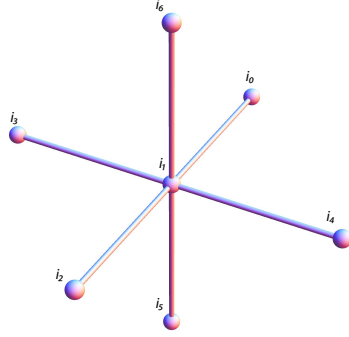


Figure 1. In our convention a gauge transformation g at location i_1 transforms $U_{i_1 i_2} \rightarrow gU_{i_1 i_2}$, $U_{i_1 i_4} \rightarrow gU_{i_1 i_4}$, $U_{i_1 i_6} \rightarrow gU_{i_1 i_6}$, $U_{i_0 i_1} \rightarrow U_{i_0 i_1} g^{-1}$, $U_{i_3 i_1} \rightarrow U_{i_3 i_1} g^{-1}$, $U_{i_5 i_1} \rightarrow U_{i_5 i_1} g^{-1}$.

To conclude we give a simple expression for the modular S -matrix that can be obtained by calculating the trace of the monodromy matrix

$$S_{(A,\alpha)(B,\beta)} = \frac{1}{|H|} \sum_{g \in A, h \in B, [g,h]=e} \text{Tr}_\alpha(x_g^{-1} h x_g)^* \text{Tr}_\beta(x_h^{-1} g x_h)^*, \quad (22)$$

where $[g, h]$ is the group theoretical commutator: $[g, h] = ghg^{-1}h^{-1}$.

2.2. Lattice actions and observables

We discretize three-dimensional spacetime into a set of sites i, j, \dots using a rectangular lattice. The gauge field U_{ij} , which takes values in the gauge group H , lives on the links ij, jk, \dots connecting sets of neighboring sites. The links are oriented in the sense that $U_{ij} = U_{ji}^{-1}$ [17].

We note that the gauge field U_{ij} takes care of the parallel transport of matter fields that are charged under the gauge group from site i to site j . An ordered product of links along a closed loop is gauge invariant up to conjugation by a group element and measures the holonomy of the gauge connection. Gauge transformations are labeled by a group element $g_i \in H$ and are performed at the sites of the lattice. The gauge field transforms as

$$U_{ij} \mapsto g_i U_{ij} g_j^{-1}, \quad (23)$$

where the orientation of the links (incoming or outgoing) has to be taken into account as shown in Figure 1.

The standard form for the lattice gauge field action makes use of the ordered product of links around a plaquette $ijkl$:

$$U_p = U_{ijkl} = U_{ij} U_{jk} U_{kl} U_{li},$$

which transforms under conjugation by the gauge group,

$$U_p \mapsto g_i U_p g_i^{-1}.$$

The gauge action per plaquette which corresponds to the Yang-Mills form $F_{\mu\nu}^2$ in the continuum limit for $H = SU(N)$ [17], is given by

$$S_p = - \sum_{\alpha} \beta_{\alpha} \chi_{\alpha}(U_p) , \quad (24)$$

where χ_{α} is the group character in irrep α and β_{α} is inversely proportional to the square of the coupling constant for irrep α . The action (24) is the euclidean analog of the Kitaev Hamiltonian introduced in [18] (which in itself is a variation of the Kogut-Susskind Hamiltonian [19]) where the role of the “star” operators is taken over by the timelike plaquettes.

For $SU(N)$ gauge theories one usually only includes the fundamental representation and is thus left with only one coupling constant. This is not necessary however: gauge invariance of the action is ensured by the fact the characters are class functions, in and therefore we will consider actions where the number of independent couplings equals the number of classes i.e. the number of irreps (for a finite group these numbers are finite and equal).

For our purposes, equation (24) is not the most convenient to work with. We perform a change of basis in the space of coupling constants to write it as a sum over delta functions on classes: $\delta_A(h) = 1$ if $h \in A$, and 0 otherwise. In this basis the action becomes

$$S_p = - \sum_A \beta_A \delta_A(U_p) .$$

This formulation allows us in particular to directly control the ”mass” of the different fluxes in the theory, which will ease the search for different vacua in the phase diagram. To perform the transformation to the class basis, we need to make use of the following orthogonality relations valid for all finite groups H

$$\int_H dg \chi_{\alpha}(g) \chi_{\beta}^*(g) = \delta_{\alpha,\beta} , \quad (25)$$

$$\begin{aligned} \sum_{\alpha \in \mathcal{R}} \chi_{\alpha}(g) \chi_{\alpha}^*(h) &= \frac{|H|}{|A|} \text{ if } g, h \in A \\ &= 0 \text{ otherwise,} \end{aligned} \quad (26)$$

where $|H|$ is the order of the group H , $|A|$ is the order of the class A , \mathcal{R} is the set of irreps and group integration is defined as

$$\int_H dg f(g) = \frac{1}{|H|} \sum_{g \in H} f(g) .$$

Equations (25) and (26) show that the irreducible representations of a group H form an orthonormal set for functions on classes of H . We thus expect the class delta function to be expressible in terms of characters

$$\delta_A(g) = \sum_{\alpha \in \mathcal{R}} c_{\alpha} \chi_{\alpha}(g) ,$$

for some set of constants $\{c_\alpha\}$. We multiply both sides of this expression by a character of the same group element in another irrep β and perform the integrations by use of the orthogonality relations (25) and (26)

$$\int_H dg \chi_\beta^*(g) \delta_A(g) = \sum_{\alpha \in \mathcal{R}} c_\alpha \int_H dg \chi_\beta^*(g) \chi_\alpha(g),$$

$$\frac{|A|}{|H|} \chi_\beta^*(A) = \sum_{\alpha \in \mathcal{R}} c_\alpha \delta_{\alpha\beta} = c_\beta,$$

where the slightly abusive notation $\chi_\alpha(A)$ means the character of any group element of A in the representation α . This shows that

$$\delta_A(g) = \sum_{\alpha \in \mathcal{R}} \frac{|A|}{|H|} \chi_\alpha^*(A) \chi_\alpha(g), \quad (27)$$

which in turn implies that the the difference between (24) and (2.2) is just a change of basis:

$$\sum_{A \in \mathcal{C}} \beta_A(\beta_\alpha) \delta_A(g) = \sum_{\alpha \in \mathcal{R}} \beta_\alpha \chi_\alpha(g),$$

where \mathcal{C} is the set of conjugacy classes and $\beta_A(\beta_\alpha)$ is given by

$$\beta_A = \sum_{\alpha} \beta_\alpha \chi_\alpha(A).$$

To probe the physics of the system for a fixed set of values of the coupling constants in the action, we will use a set of order parameters and phase indicators. These order parameters are in one-to-one with the set of fundamental anyonic excitations of the theory.

Order parameters and phase indicators. We distinguish two different sets of order parameters that are closely related to one another. The first is the set of closed *loop operators*, that physically correspond to the creation, propagation and annihilation of a anyon-anti-anyon pair in spacetime. The second is the set of open *string operators* that create, propagate and annihilate a single anyon. In the background of a trivial vacuum, only the loops can have nonzero expectation values, since the creation of a single particle would violate the conservation of the quantum numbers of the vacuum in such a background. This means that the open strings tell us something about possible Bose condensates, whereas the closed loops tell us about the behaviour of external particles put into this background. We define the open string operators only for the purely magnetic sectors, since in this work we only study magnetic condensates.

First we will define the loop operators. This set of nonlocal order parameters was introduced in a previous publication [20]. For a full discussion, we refer to that work. Here we recall the essentials and fix the notation. The closed loops are a generalization of the Wilson and 't Hooft loops. They create a particle-antiparticle pair from the vacuum and annihilate them at a later time. These loops allow us to calculate Aharonov-Bohm type phases and check for confinement of certain anyonic excitations. In $SU(N)$ gauge

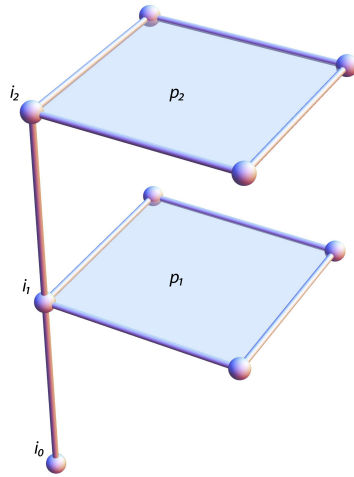


Figure 2. The first two plaquettes appearing in expression (28). The ordered product U_p of links around a plaquette p needs to be taken with an orientation that has to be constant throughout the loop.

theories, the Wilson loop for a free excitations in general falls off as e^{-cP} , with P the perimeter of the loop, whereas a confined excitation falls off as $e^{-c'A}$, with A the area of the loop. We find that in the DGT the expectation values of loop operators are in general independent of the size of the loops as it should be, given that the lattice is large enough to accomodate the operators in such a way that they stay away a few lattice spacings from the edges. Single loops for unconfined particles give the value of the quantum dimension whereas loops for confined particles evaluate to zero. A combination of two loops that link allow us to measure the elements of the modular S -matrix. The different fluxes in a conjugacy class A are called h_i . We pick a basepoint i_0 in spacetime that serves as a reference point at which location fluxes can be compared. We want to insert extra flux in a set of plaquettes in a gauge invariant manner.

In order to achieve this we change the Boltzmann factor for the plaquettes involved to one that favors this particular flux; this is most easily understood by an example. Suppose the set of coupling constants β_A is chosen such that the trivial vacuum is realized. This means that nearly all plaquettes will have the value $U_p = e$, the identity element of the group, so the plaquette action $S(U_p)$ will have a minimum for $U_p = e$. If we change the action for a certain set of plaquettes from $S(U_p)$ to $S(h^{-1}U_p)$, the minimum has changed from $U_p = e$ to $U_p = h$, so by “twisting” the action for a given plaquette with a group element h^{-1} , we insert a flux h .

The group element that needs to be used for the twist will vary from site to site and the one to be inserted into the action at plaquette p_j is denoted by $h_i^{p_j}$. For example, if we want to insert a flux h at a location connected to i_0 by the gauge connection U_{01} , this group element would be $U_{01}^{-1} h^{-1} U_{01}$. We then change the action for this plaquette from $S(U_p)$ to $S(U_{01}^{-1} h^{-1} U_{01} U_p)$. If we now draw a closed loop on the dual lattice, this loop pierces a set of plaquettes. Such a set can be seen in Figure 3, which is included to

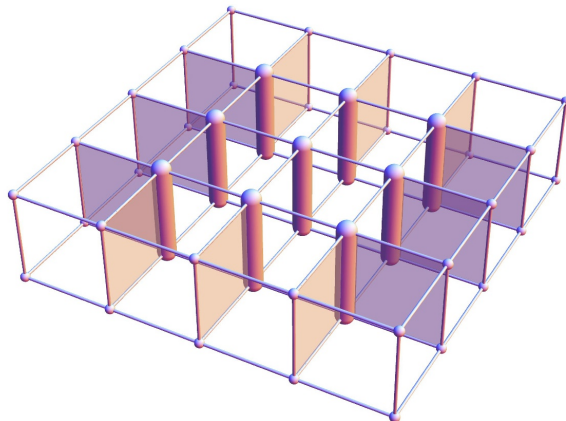


Figure 3. A set of plaquettes forming a closed loop on the lattice. The fat links constitute the h -forest.

give an intuition on the type of gauge field configurations contributing to the partition sum once extra flux has been inserted. In this figure we have multiplied all the fat links (dubbed the h -forest by [21]) with a group element h , resulting in a loop of h -flux. In the trivial vacuum, this configuration (modulo gauge transformations) makes the dominant contribution to the partition sum.

We call the set of plaquettes Ξ . With this notation and the above considerations, the anyonic operator $\Delta^{(A,\alpha)}$ is given by ‡:

$$\Delta^{(A,\alpha)}(\Xi) = \sum_{h_i \in A} \prod_{p_j \in \Xi} D_\alpha \left(x_{U_{j-1,j}^{-1} h_i^{p_j} U_{j-1,j}^{-1}}^{-1} U_{j-1,j} x_{h_i^{p_j}} \right) e^{S(U_{p_j}) - S(h_i^{p_j} U_{p_j})}. \quad (28)$$

Here p_j iterates over the plaquettes in Ξ and D_α is the representation function of the centralizer irrep α . The link $U_{j-1,j}$ neighbours the plaquette p_j , and the combination in brackets always takes values in the centralizer subgroup of the class A . The exponential of the difference of two actions changes the minimal action configuration to one containing flux h_i for the plaquette under consideration.

The operator in expression (28) is a generalization of the Wilson and 't Hooft loops. If we fill in for A the trivial class, the exponent vanishes and the x group elements are equal to the group unit, so after we multiply out the D_α -matrices we are left with

$$\Delta^{(e,\alpha)}(\Xi) = \chi_\alpha (U_{1,2} U_{2,3} \cdots U_{n-1,n} U_{n,1}),$$

where the product of U s is an ordered product along the loop on the lattice.

On the other hand, if we replace α by the trivial representation, we are left with

$$\Delta^{(A,1)}(\Xi) = \sum_{h_i \in A} \prod_{p_j \in \Xi} e^{S(U_{p_j}) - S(h_i^{p_j} U_{p_j})},$$

which is comparable to the order parameter proposed in [21], but the gauge invariance with respect to the transformations (23) is ensured in a different way. We sum over the

‡ This definition is different from our original definition [20] by a factor of $\frac{1}{|A|}$. This definition gives the correct S -matrix elements directly.

conjugacy class only once and insert the flux in a gauge invariant matter by parallel transporting it along the loop from a fixed basepoint. The operator in [21] sums over the conjugacy class for each individual plaquette. This way also gauge invariance is achieved, but the loop loses its orientation, and therefore can never carry anyonic charge.

The open magnetic string operators are a variant of expression (28) where the set of plaquettes Ξ corresponds to an open string on the dual lattice. Looking at the h -forest configurations, it can immediately be seen that such a string, corresponding to the creation and subsequent annihilation of a single particle, has zero expectation value in the trivial vacuum. For these strings to acquire a non zero expectation value a *vacuum exchange contribution* is required, which we will focus on now.

The vacuum exchange contribution. We use the set of operators $\{\Delta^{(A,\alpha)}\}$ to measure the elements of the S -matrix by picking two loops Ξ_1 and Ξ_2 that link each other once

$$\langle S_{(A,\alpha)(B,\beta)} \rangle = \langle \Delta^{(A,\alpha)}(\Xi_1) \Delta^{(B,\beta)}(\Xi_2) \rangle. \quad (29)$$

In the trivial vacuum the $S_{(A,\alpha)(B,\beta)}$ -matrix elements of fluxes $g \in A$ and $h \in B$ for which $g h g^{-1} h^{-1} = [g, h] \neq e$ evaluate to zero (this is what we measure using the operators (28) and calculate algebraically (22)). If we however measure the S -matrix elements of such noncommuting fluxes in a broken vacuum nonzero matrix elements can appear.

This is most easily explained by considering an example. The main contribution to a single loop of pure magnetic flux is of the form pictured in Figure 3. This configuration is called the h -forest state in earlier literature [21]. Modulo gauge transformations this is the dominant configuration in the trivial vacuum that contributes to a loop of flux labeled by conjugacy class A , where $g \in A$. Expression (28) contains a sum over these group elements within a class, but let us for now focus on one of the group elements. Each link in this configuration has value e , except for the fat links in Figure 3, they have value h . That this configuration leads to a loop or tube of flux is easily seen: within the forest each plaquette has a value $e h e h^{-1} = e$, whereas at the edges the value is $e h e e = h$ (depending on the orientation of the plaquette product). This is also the easiest way to see the origin of the Aharonov-Bohm effect on the lattice: an electric charge loop having linking number 1 with the flux loop will have exactly one link with value h in it, therefore its value will be $\chi_\alpha(h)$.

Consider now the dominant configuration that contributes to the S -matrix element $S_{(A,1)(B,1)}$. We again pick two group elements $g \in A$, $h \in B$ and draw a similar diagram. This is shown in Figure 4. By similar logic this causes the plaquettes at the boundary of either forest to have value g respectively h . Inside the forests most plaquettes still have value e , however there are some plaquettes that are different. There is a tube of plaquettes that have value $[g, h]$, where the two forests intersect. In general this group theoretical commutator is not equal to identity element for nonabelian groups. This is the physical reason behind the appearance of zeroes in the S -matrix for nonabelian theories. This tube of plaquettes represents a flux $[g, h]$ going from the one loop to the other. In the trivial vacuum this flux will be gapped, so the contribution of this diagram

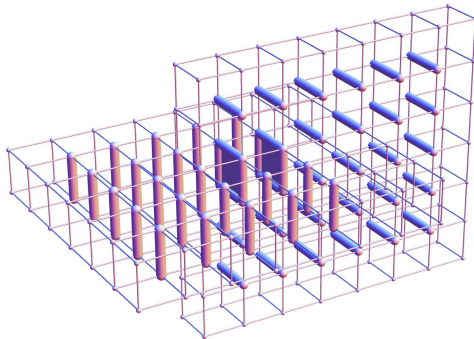


Figure 4. The vacuum exchange contribution. Double h -forest, configuration contributing to the S -matrix measurement of two non commuting fluxes. The fat links are the g -forest and h -forest and the shaded plaquettes are a string of $[g, h]$ flux connecting the the two loops.

to the path integral expectation value will be negligible.

However, a different situation appears when we are in a vacuum where the flux $[g, h]$ has Bose condensed. We cannot give a single configurations that contributes dominantly to the path integral (there are many), but we can say that configurations like the one in Figure 4 are now contributing since the mass for the flux $[g, h]$ has disappeared.

Thus we expect that in the measurements there will be cases where zeroes in the original S -matrix will obtain a nonzero value in the broken phase.

An auxiliary $^A N$ gauge symmetry. The operators (28) are invariant with respect to the local H gauge transformations (23). However, in our formulation of the operators we have tacitly introduced another, auxiliary $^A N$ gauge symmetry that is less obvious. A crucial property that allows one to determine the topological symmetry breaking pattern in detail is that the loop operators do transform nontrivially under this symmetry. In a non trivial ground state, these symmetries may be broken and will therefore lead to the lifting of certain degeneracies related with the splitting of fields in the topological symmetry breaking process. So this hidden symmetry turns out to be a blessing in disguise.

Let us first note that there is no preferred choice for the coordinate system (19) we define for the conjugacy classes. Once a certain choice $\{x_{h_i}\}$ has been made such that $h_i = x_{h_i} h_1 x_{h_i}^{-1}$, a set $\{x'_{h_i}\}$ with

$$x'_{h_i} = x_{h_i} n_{h_i}, \quad [n_{h_i}, h_i] = e, \quad (30)$$

will do just as well. In the trivial vacuum, the S -matrix is invariant with respect to this transformation. This is most easily seen by looking at the algebraic expression (22), but it is also confirmed by our measurements of (29).

This invariance can be understood on the operator level by multiplying out the representation matrices of the centralizer in equation (28). Generally this will lead to terms of the form

$$\mathrm{Tr}_\alpha \tilde{g} = \mathrm{Tr}_\alpha (x_{h_k}^{-1} g x_{h_i}),$$

where g is the product of links on the loop and $h_k = g h_i g^{-1}$, implying that indeed $\tilde{g} \in {}^A N$. When the loop is linked with another loop, the element g will in general be in the conjugacy class of the flux of this other loop. Under the transformation (30) of the class coordinate system, the above expression will transform as

$$\mathrm{Tr}_\alpha (n_{h_k}^{-1} x_{h_k}^{-1} g x_{h_i} n_{h_i}) = \mathrm{Tr}_\alpha (n_{h_i} n_{h_k}^{-1} x_{h_k}^{-1} g x_{h_i}),$$

due to the cyclicity of the trace. This elucidates the invariance of the S -matrix in the trivial vacuum under the translation of the x_{h_i} : non-commuting fluxes never have a non-zero matrix element, and if $[g, h] = e$, we have that $h_i = h_k$ and therefore $n_{h_i} n_{h_k}^{-1} = e$. In a non-trivial ground state where non-commuting fluxes may have non-zero S -matrix elements due to a vacuum interchange contribution, the transformation (30) may manifest itself in different measured matrix elements. This means that in such cases the entry (A, α) may split into multiple entries $\{(A_i, \alpha_i)\}$. As we are interested in these multiple entries, we will in our calculations always include the nontrivial behavior of our observables under this auxiliary ${}^A N$ action. This turns out to be one of two mechanisms responsible for the splitting of irreps of \mathcal{A} into multiple irreps of \mathcal{U} , the other of which we turn to now.

An auxiliary $H/{}^A N$ symmetry. There is another symmetry, but now on the level of the fusion algebra that turns out to be useful. Suppose in the theory there exists a rule of the form

$$(A, \alpha) \times (e, \beta) = (A, \alpha), \quad (31)$$

where (e, β) is some one-dimensional purely electric representation. This turns out to be the case whenever the representation $\Pi^{(e, \beta)}(\cdot)$ evaluates to unity for all elements in ${}^A N$, the normalizer of class A . We can prove this using the explicit expression for the fusion coefficients in terms of the quantum double characters:

$$N_{(C, \gamma)}^{(A, \alpha)(B, \beta)} = \frac{1}{|H|} \sum_{g, h} \mathrm{Tr} [\Pi^{(A, \alpha)} \otimes \Pi^{(B, \beta)} (\Delta(P_h g))] \mathrm{Tr} [\Pi^{(C, \gamma)} (P_h g)]^*. \quad (32)$$

Picking $(B, \beta) = (e, \beta)$ and $(C, \gamma) = (A, \alpha)$,

$$\begin{aligned} N_{(A, \alpha)}^{(A, \alpha)(e, \beta)} &= \frac{1}{|H|} \sum_{g, h} \mathrm{Tr} \left[\Pi^{(A, \alpha)} \otimes \Pi^{(e, \beta)} \left(\sum_{h_1 h_2 = h} P_{h_1} g \otimes P_{h_2} g \right) \right] \cdots \\ &\quad \cdots \mathrm{Tr} [\Pi^{(A, \alpha)} (P_h g)]^* \\ &= \frac{1}{|H|} \sum_{g, h} \mathrm{Tr} [\Pi^{(A, \alpha)} (P_h g) \otimes \Pi^{(e, \beta)} (P_e g)] \mathrm{Tr} [\Pi^{(A, \alpha)} (P_h g)]^* \\ &= \frac{1}{|H|} \sum_{g \in {}^A N, h \in A} \mathrm{Tr} [\Pi^{(A, \alpha)} (P_h g)] \mathrm{Tr} [\Pi^{(A, \alpha)} (P_h g)]^* = 1, \end{aligned}$$

where in the latter line we have made use of the orthogonality of the characters. We assumed $\Pi^{(e,\beta)}(P_e g) = 1$ for all $g \in {}^A N$. The sum over h is restricted since if $h \notin A$ the matrix element will be zero and the sum over g is restricted since if $g \notin {}^A N$ the matrix element will be off-diagonal and thus not contribute to the trace.

So it seems that the fusion rule (31) leads a degeneracy in the calculation of S -matrix elements since by definition

$$\left\langle \begin{array}{c} \text{Diagram: Two circles, left labeled } (A,\alpha) \text{ and right labeled } (C,\gamma). \end{array} \right\rangle_0 = \left\langle \begin{array}{c} \text{Diagram: A vertical line with three loops. Top loop labeled } (A,\alpha), \text{ middle loop labeled } (e,\beta), \text{ bottom loop labeled } (C,\gamma). \end{array} \right\rangle_0.$$

However, on the operator level this equality does not hold. Indeed, when we probe the LHS of this equation in a non-trivial vacuum the result will in general differ from the RHS. In particular, it turns out that the different \mathcal{U} representations that lift to the same \mathcal{A} representations (A, α) differ precisely by such a fusion. So this degeneracy may be lifted in the broken phase and give rise to a additional splittings of certain entries (A, α) . Consequently in our numerical calculations we have to explicitly keep track of the presence of such electric representations (e, β) , that satisfy (31) and see whether they give rise to additional splittings.

To conclude this section, we remark that we have very explicitly indicated how one gets from the modular S -matrix S_{ab} to the extended or broken S -matrix $\bar{S}_{a_i b_j}$, from which the topological data of the broken \mathcal{U} phase can be immediately read off.

3. The $D(\bar{D}_2)$ gauge theory

We turn to the particular example we have chosen to work out in detail: a discrete gauge theory with gauge group \bar{D}_2 , also called the quaternion group. The representation theory was worked out in [16], here we summarize the results that are required to describe the breaking by a Bose condensate.

3.1. Algebraic analysis

The group \bar{D}_2 contains eight elements that can be represented by the set of 2×2 -matrices

$$\{\mathbf{1}, -\mathbf{1}, \pm i\sigma_1, \pm i\sigma_2, \pm i\sigma_3\}, \quad (33)$$

where the σ_i , $i = 1, 2, 3$ are the Pauli spin matrices. We denote the conjugacy classes as $e = \{\mathbf{1}\}$, $\bar{e} = \{-\mathbf{1}\}$, $X_1 = \{i\sigma_1, -i\sigma_1\}$, $X_2 = \{i\sigma_2, -i\sigma_2\}$, $X_3 = \{i\sigma_3, -i\sigma_3\}$ and the irreducible group representations as 1, the trivial irrep, J_1 , J_2 , J_3 three one-dimensional irreps and χ the two-dimensional irrep given by (33). The character table is given on the left hand side of Table 1. The centralizer groups for the classes e and \bar{e} are both \bar{D}_2 since the elements in these classes constitute the center of the group. The classes X_i , $i = 1, 2, 3$ have non-trivial \mathbb{Z}_4 centralizer subgroups, of which the character table is given on the right hand side of Table 1. The irreducible representations of the quantum

\bar{D}_2	e	\bar{e}	X_1	X_2	X_3	\mathbb{Z}_4	$\mathbb{1}$	$i\sigma_i$	$-\mathbb{1}$	$-i\sigma_i$
1	1	1	1	1	1	Γ^0	1	1	1	1
J_1	1	1	1	-1	-1	Γ^1	1	i	-1	$-i$
J_2	1	1	-1	1	-1	Γ^2	1	-1	1	-1
J_3	1	1	-1	-1	1	Γ^3	1	$-i$	-1	i
χ	2	-2	0	0	0					

Table 1. Character table of the group \bar{D}_2 and of \mathbb{Z}_4 as a centralizer of the class X_i .

double are labeled by a combination (A, α) of a conjugacy class A and a centralizer irrep α . The full set of fusion rules for the $D(\bar{D}_2)$ theory is given in Appendix A. All in all, there are 22 sectors: the trivial flux paired with the five irreps of \bar{D}_2 , the \bar{e} flux paired with the five irreps of \bar{D}_2 and the three X_i fluxes paired with the four \mathbb{Z}_4 irreps. The sectors that involve an X_i flux or a χ irrep have quantum dimension 2, the others have unit quantum dimension. One obtains that the total quantum dimension for the theory $D_A = 8$.

Breaking: $(\bar{e}, 1)$ condensate. In this case the lift of the new vacuum is $\phi = (e, 1) + (\bar{e}, 1)$, which implies that $q = d_{(e,1)} + d_{(\bar{e},1)} = 2$. To determine the effective low energy theory we fuse ϕ with all particle sectors of the theory and look for the irreducible combinations that appear.

$$\begin{aligned}
 \phi \times (e, 1) &= (e, 1) + (\bar{e}, 1) \\
 \phi \times (e, J_i) &= (e, J_i) + (\bar{e}, J_i) \\
 \phi \times (e, \chi) &= (e, \chi) + (\bar{e}, \chi) \quad (*) \\
 \phi \times (\bar{e}, 1) &= (e, 1) + (\bar{e}, 1) \\
 \phi \times (\bar{e}, J_i) &= (e, J_i) + (\bar{e}, J_i) \\
 \phi \times (\bar{e}, \chi) &= (e, \chi) + (\bar{e}, \chi) \quad (*) \\
 \phi \times (X_i, \Gamma^0) &= (X_i, \Gamma^0) + (X_i, \Gamma^0) \\
 \phi \times (X_i, \Gamma^1) &= (X_i, \Gamma^1) + (X_i, \Gamma^3) \quad (*) \\
 \phi \times (X_i, \Gamma^2) &= (X_i, \Gamma^2) + (X_i, \Gamma^2) \\
 \phi \times (X_i, \Gamma^3) &= (X_i, \Gamma^1) + (X_i, \Gamma^3) \quad (*)
 \end{aligned}$$

The lines marked with (*) have components on the right hand side that carry different spin factors, implying that they are confinement in the broken phase. Studying the fusion rules of the surviving combinations of irreps leads to the conclusion that the effective \mathcal{U} theory is $D(\mathbb{Z}_2 \otimes \mathbb{Z}_2)$. This means $\mathcal{D}_{\mathcal{T}}^2 = 32$ and $\mathcal{D}_{\mathcal{U}}^2 = 16$. The branchings of \mathcal{A} irreps into the unconfined \mathcal{U} theory are

$$\begin{aligned}
 (e, 1) + (\bar{e}, 1) &\rightarrow (++, ++), \quad d_{(++++)} = 1 \\
 (e, J_1) + (\bar{e}, J_1) &\rightarrow (++, +-), \quad d_{(+++-)} = 1 \\
 (e, J_2) + (\bar{e}, J_2) &\rightarrow (++, -+), \quad d_{(++-+)} = 1
 \end{aligned}$$

$$\begin{aligned}
(e, J_3) + (\bar{e}, J_3) &\rightarrow (++, --), & d_{(++,-)} &= 1 \\
(X_1, \Gamma^0)_1 &\rightarrow (-+, ++), & d_{(-+,++)} &= 1 \\
(X_1, \Gamma^0)_2 &\rightarrow (-+, +-), & d_{(-+,+-)} &= 1 \\
(X_1, \Gamma^2)_1 &\rightarrow (-+, -+), & d_{(-+,-+)} &= 1 \\
(X_1, \Gamma^2)_2 &\rightarrow (-+, --), & d_{(-+,-)} &= 1 \\
(X_2, \Gamma^0)_1 &\rightarrow (+-, ++), & d_{(+-,++)} &= 1 \\
(X_2, \Gamma^0)_2 &\rightarrow (+-, -+), & d_{(+-,+-)} &= 1 \\
(X_2, \Gamma^2)_1 &\rightarrow (+-, +-), & d_{(+-,+-)} &= 1 \\
(X_2, \Gamma^2)_2 &\rightarrow (+-, --), & d_{(+-,--)} &= 1 \\
(X_3, \Gamma^0)_1 &\rightarrow (--, ++), & d_{(--,++)} &= 1 \\
(X_3, \Gamma^0)_2 &\rightarrow (--, --), & d_{(--,-)} &= 1 \\
(X_3, \Gamma^2)_1 &\rightarrow (--, +-), & d_{(--,+-)} &= 1 \\
(X_3, \Gamma^2)_2 &\rightarrow (--, -+), & d_{(--,-+)} &= 1
\end{aligned}$$

which all have quantum dimension $d_u = 1$, while the confined fields are

$$\begin{aligned}
(e, \chi) + (\bar{e}, \chi) &\rightarrow t_1, & d_{t_1} &= 2 \\
(X_1, \Gamma^1) + (X_1, \Gamma^3) &\rightarrow t_2, & d_{t_2} &= 2 \\
(X_2, \Gamma^1) + (X_2, \Gamma^3) &\rightarrow t_3, & d_{t_3} &= 2 \\
(X_3, \Gamma^1) + (X_3, \Gamma^3) &\rightarrow t_4, & d_{t_4} &= 2
\end{aligned}$$

and have $d_t = 2$.

Breaking: (X_1, Γ^0) condensate. There is an obvious symmetry in the fusion rules between the three (X_i, Γ^0) particle sectors. We choose to study the case where the (X_1, Γ^0) condenses. This gives for the new vacuum $\phi = (e, 1) + (\bar{e}, 1) + (X_1, \Gamma^0)$, from which follows that $q = 4$ in this case. We now read off the lifts of the \mathcal{T} fields on the right:

$$\begin{aligned}
\phi \times (e, 1) &= (e, 1) + (\bar{e}, 1) + (X_1, \Gamma^0) \\
\phi \times (e, J_i) &= (e, J_i) + (\bar{e}, J_i) + \delta_{1i}(X_1, \Gamma^0) + \eta_{1i}(X_1, \Gamma^2) \\
\phi \times (e, \chi) &= (e, \chi) + (\bar{e}, \chi) + (X_1, \Gamma^1) + (X_1, \Gamma^3) \\
\phi \times (\bar{e}, 1) &= (e, 1) + (\bar{e}, 1) + (X_1, \Gamma^0) \\
\phi \times (\bar{e}, J_i) &= (e, J_i) + (\bar{e}, J_i) + \delta_{1i}(X_1, \Gamma^0) + \eta_{1i}(X_1, \Gamma^2) \\
\phi \times (\bar{e}, \chi) &= (e, \chi) + (\bar{e}, \chi) + (X_1, \Gamma^1) + (X_1, \Gamma^3) \\
\phi \times (X_1, \Gamma^0) &= (X_1, \Gamma^0) + (X_1, \Gamma^0) + (e, 1) + (\bar{e}, 1) + (e, J_1) + (\bar{e}, J_1) \\
\phi \times (X_1, \Gamma^1) &= (X_1, \Gamma^1) + (X_1, \Gamma^3) + (e, \chi) + (\bar{e}, \chi) \\
\phi \times (X_1, \Gamma^2) &= (X_1, \Gamma^2) + (X_1, \Gamma^2) + (e, J_2) + (\bar{e}, J_2) + (e, J_3) + (\bar{e}, J_3) \\
\phi \times (X_1, \Gamma^3) &= (X_1, \Gamma^1) + (X_1, \Gamma^3) + (e, \chi) + (\bar{e}, \chi)
\end{aligned}$$

$$\begin{aligned}
 \phi \times (X_i, \Gamma^0) &= (X_i, \Gamma^0) + (X_i, \Gamma^0) + (X_k, \Gamma^0) + (X_k, \Gamma^2) \quad (i \neq k \neq 1) \\
 \phi \times (X_i, \Gamma^1) &= (X_i, \Gamma^1) + (X_i, \Gamma^3) + (X_k, \Gamma^1) + (X_k, \Gamma^3) \\
 \phi \times (X_i, \Gamma^2) &= (X_i, \Gamma^2) + (X_i, \Gamma^2) + (X_k, \Gamma^0) + (X_k, \Gamma^2) \\
 \phi \times (X_i, \Gamma^3) &= (X_i, \Gamma^1) + (X_i, \Gamma^3) + (X_k, \Gamma^1) + (X_k, \Gamma^3)
 \end{aligned}$$

We have used the symbol δ_{ij} which is 1 when i and j are equal and is zero otherwise, and η_{ij} which is 1 when i and j are not equal and is zero when i and j are. The \mathcal{U} theory is $D(\mathbb{Z}_2) \simeq \mathbb{Z}_2 \otimes \mathbb{Z}_2$. This means $\mathcal{D}_7^2 = 16$ and $\mathcal{D}_U^2 = 4$. The lifts of the unconfined fields are:

$$\begin{aligned}
 (e, 1) + (\bar{e}, 1) + (X_1, \Gamma^0)_1 &\rightarrow (+, +), \quad d_{(+,+)} = 1 \\
 (e, J_1) + (\bar{e}, J_1) + (X_1, \Gamma^0)_2 &\rightarrow (+, -), \quad d_{(+,-)} = 1 \\
 (X_2, \Gamma^0)_1 + (X_3, \Gamma^0)_1 &\rightarrow (-, +), \quad d_{(-,+)} = 1 \\
 (X_2, \Gamma^2)_1 + (X_3, \Gamma^2)_1 &\rightarrow (-, -), \quad d_{(-,-)} = 1
 \end{aligned}$$

and of the confined fields:

$$\begin{aligned}
 (e, J_2) + (\bar{e}, J_2) + (X_1, \Gamma^2)_1 &\rightarrow t_1, \quad d_{t_1} = 1 \\
 (e, J_3) + (\bar{e}, J_3) + (X_1, \Gamma^2)_2 &\rightarrow t_2, \quad d_{t_2} = 1 \\
 (e, \chi) + (\bar{e}, \chi) + (X_1, \Gamma^1) + (X_1, \Gamma^3) &\rightarrow t_3, \quad d_{t_3} = 2 \\
 (X_2, \Gamma^0)_2 + (X_3, \Gamma^2)_2 &\rightarrow t_4, \quad d_{t_4} = 1 \\
 (X_3, \Gamma^0)_2 + (X_2, \Gamma^2)_2 &\rightarrow t_5, \quad d_{t_5} = 1 \\
 (X_2, \Gamma^1) + (X_2, \Gamma^3) + (X_3, \Gamma^1) + (X_3, \Gamma^3) &\rightarrow t_6, \quad d_{t_6} = 2
 \end{aligned}$$

3.2. Measurements by lattice Monte Carlo simulations

The five couplings $\{\beta_A\}$ for conjugacy class A that appear in the action of the $D(\bar{D}_2)$ theory

$$S_p = \sum_p - \{ \beta_e \delta_e(U_p) + \beta_{\bar{e}} \delta_{\bar{e}}(U_p) + \beta_{X_1} \delta_{X_1}(U_p) + \beta_{X_2} \delta_{X_2}(U_p) + \beta_{X_3} \delta_{X_3}(U_p) \}, \quad (34)$$

are inversely proportional to the masses of the fluxes A . For example if we put all couplings to zero except for β_e , which we make large (at least as large as 2.0 as we will see shortly), the trivial vacuum is realized: this is the configuration where for all plaquettes $U_p = e$. Deviations from this configuration occur because of quantum fluctuations, but since all excitations are gapped they will be exponentially suppressed. The gap in this vacuum is easily calculated to be of the order of $4\beta_e$, since the smallest excitation above the configuration in which all plaquettes are e is one in which one link has a value $h \neq e$. This excites four plaquettes and changes the action (34) by a value of $4\beta_e$.

Monte Carlo considerations. For the other, nontrivial phases in this theory, the dominant configurations contributing to the path integral are not so readily identified. To gain insight into what configurations contribute we use a Monte Carlo simulation,

in particular a modified *heat bath* algorithm. Bluntly applying this algorithm to our problem leads to various complications, therefore we briefly point out the method, the complications and how we have resolved them.

The procedure starts with some initial configuration of link variables $\{U\}_1$. We then update all links in lexicographic order, a process called a sweep, and arrive at a new configuration $\{U\}_2$. The updating process for each link proceeds as follows. Consider the link U_{ij} . We identify which plaquettes contain this link: in three dimensions, there are four such plaquettes. Now we calculate, for each element $g \in H$, what the sum of the plaquette actions for each of these four plaquettes would be if U_{ij} were to have the value g . This gives a set of numbers

$$\{S_{g_1}, S_{g_2}, \dots, S_{g_{|H|}}\},$$

where S_{g_k} is the sum of the four plaquette actions with U_{ij} equal to g_k . We now calculate a localized partition sum $Z_{U_{ij}}$:

$$Z_{U_{ij}} = \sum_{g \in H} e^{-S_g},$$

which can be used to calculate a set of probabilities $\{p(g)\}_{g \in H}$ for each group element g

$$p(g) = \frac{e^{-S_g}}{Z_{U_{ij}}}.$$

After a given number of sweeps n_0 , the Monte Carlo algorithm arrives at the minimum of the action and the path integral expectation value of the operator O

$$\langle O \rangle = \frac{\int DU O[U] e^{-S[U]}}{\int DU e^{-S[U]}} \quad (35)$$

is given by taking the average of $O[\{U\}_n]$, the value of O at gauge field configuration $\{U\}_n$:

$$\langle O \rangle_{\text{MC estimate}} = \frac{1}{m} \sum_{n=n_0+1}^{n_0+m} O[\{U\}_n]. \quad (36)$$

However, for our purposes this scheme is troublesome for two reasons: it is tacitly assumed that the presence of the operator O in (35) does not change the value of the minimum of the action S and furthermore the loops of magnetic flux are very non-local objects and therefore highly unlikely to appear when using a local updating algorithm. This is illustrated in Figure 5. The shift upward of the functional $S[U]$ is due to the presence of a magnetic flux string and the shift to the left is due to the non-locality of the magnetic excitations. The latter shift also occurs when a single loop of flux is inserted.

The minimum of the action in the calculation of an S -matrix element (29) is altered by the insertions of the loop operators: the configuration for two non-commuting fluxes carries a string (see the discussion around Figure 4) that is massive and thus costs a finite amount of action. There is no way to get rid of this string and therefore the

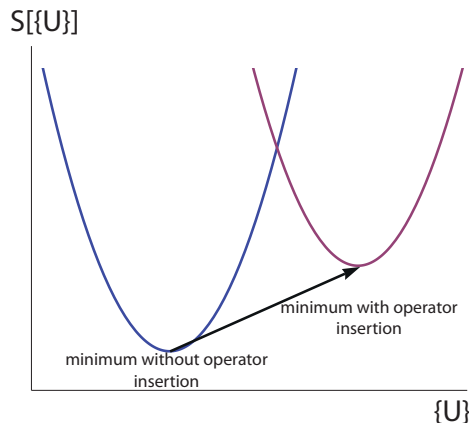


Figure 5. Schematic drawing of the action as a functional of the gauge field configuration $\{U\}$. The insertion of non-commuting fluxes shifts the minimum of the action to a different location in the configuration space (due to the non-local nature of the excitations) and to a different value (due to the presence of a string).

minimum value of the action in the presence of the two loops is shifted. We therefore have to amend the standard MC algorithm. Defining

$$\begin{aligned} S &= S_{\min} + \delta S \quad \text{without operator insertion,} \\ \tilde{S} &= \tilde{S}_{\min} + \delta \tilde{S} \quad \text{with operator insertion,} \end{aligned}$$

and noticing that around the minimum the actions behave identically, implying that δS and $\delta \tilde{S}$ are the same functions, expression (35) becomes

$$\langle O \rangle = \frac{\int DU e^{-(\tilde{S}_{\min} - S_{\min})} O[U] e^{-\delta S[U]}}{\int DU e^{-\delta S[U]}}. \quad (37)$$

This leads to a modified Monte Carlo average

$$\langle O \rangle_{\text{MC estimate}} = \frac{1}{m} e^{-(\tilde{S}_{\min} - S_{\min})} \sum_{n=n_0+1}^{n_0+m} O[\{U\}_n]. \quad (38)$$

We now describe two approaches to the second problem in our MC measurements: the low probability that the local updating algorithm will converge to a gauge field configuration containing a (set of) magnetic flux loop(s). We will assume a single loop of pure magnetic flux is inserted, as nothing substantial will change in the case of multiple loops or the addition of dyonic charge.

The first approach is based on the observation, illustrated in Figure 3, that we know the gauge field configuration (up to gauge transformations) that extremizes the action in the trivial vacuum with the insertion of a loop of magnetic flux: the h -forest. We can therefore use this configuration as an *ansatz* in the MC algorithm. We start with a “cold lattice”, all links $U_{ij} = e$, except for the h -forest, for these links we set $U_{ij} = h$. This is an extremum of the action for the action if we set all $\beta_{A \neq e} = 0$ and $\beta_e \gg 1$. To perform a measurement at some other value of the coupling constants, we can slowly change the coupling constants towards the desired values, performing a few MC updates after each

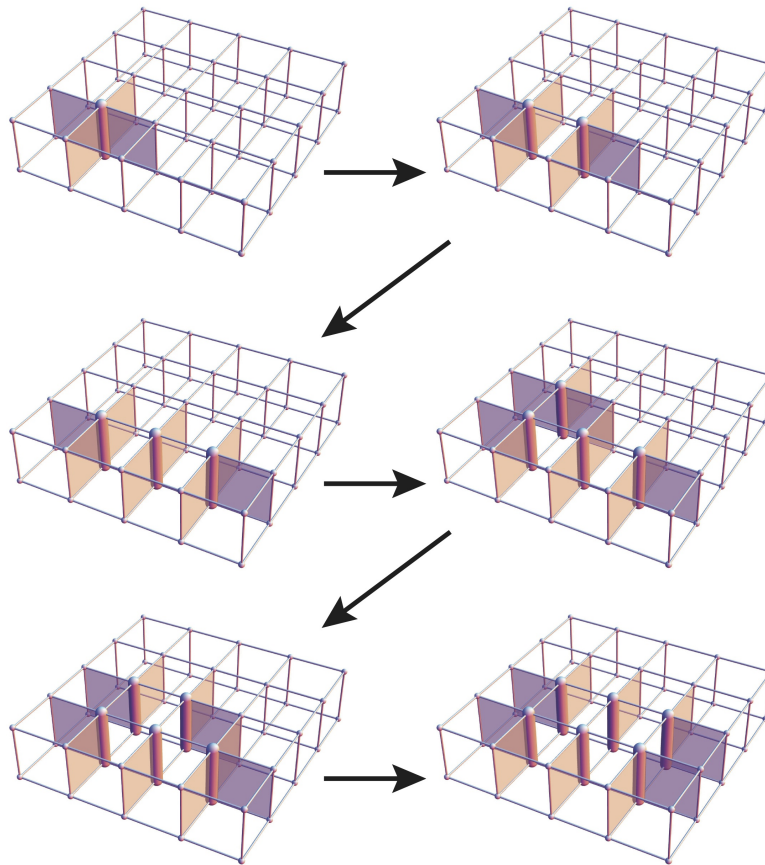


Figure 6. Growing a flux loop in multiple steps. The shaded plaquettes have a twisted action, and the fat links show the convergence towards a h -forest state.

step. The second approach is a more physical one. We initialize the lattice directly at the desired point in coupling constant space. The trick is then not to insert the loop all at once, but to slowly grow it, as illustrated in Figure 6. We start by twisting the action for four plaquettes around one link, as shown by the shaded plaquettes in the top left of Figure 6. After this, a number of MC updates are performed. Then the set of plaquettes that have a twisted action is changed as in the top right corner of the Figure. Again a number of MC updates is performed and so on. We have checked that in the trivial vacuum one obtains the h -forest configuration using this procedure. Both of methods to insert flux loops have been used by us and we have verified that they lead to completely equivalent results.

3.3. Results

In this subsection we present the results of our Monte Carlo simulations. The first quantity we measured was the free energy as a means to map out a suitable subspace of the parameter space. It gives us an indication of the validity of our naive intuition about where nontrivial condensates should occur.

Once we have found some region where symmetry breaking occurs we measure the open string expectation values to determine the respective condensates. After that we measure the unbroken and broken S -matrix elements. Using the straightforward algorithm involving the auxiliary symmetries of our loop operators discussed in section 2.2, allows us to find the branching matrix $n_u^{a_1}$ as well as the S -matrix of the effective \mathcal{U} theory in the broken phase.

Mapping out the phase diagram. The space of coupling constants in our theory is five-dimensional but it is not our goal to analyse it completely. We have restricted our search to some representative regions where nontrivial condensates do indeed occur. To study the location of the corresponding phase transitions we measured the free energy F , which we define as the expectation value of the plaquette action, averaged over the spacetime lattice. The left plot of Figure 7 shows F as a function of $(\beta_e$ and $\beta_{\bar{e}})$ and

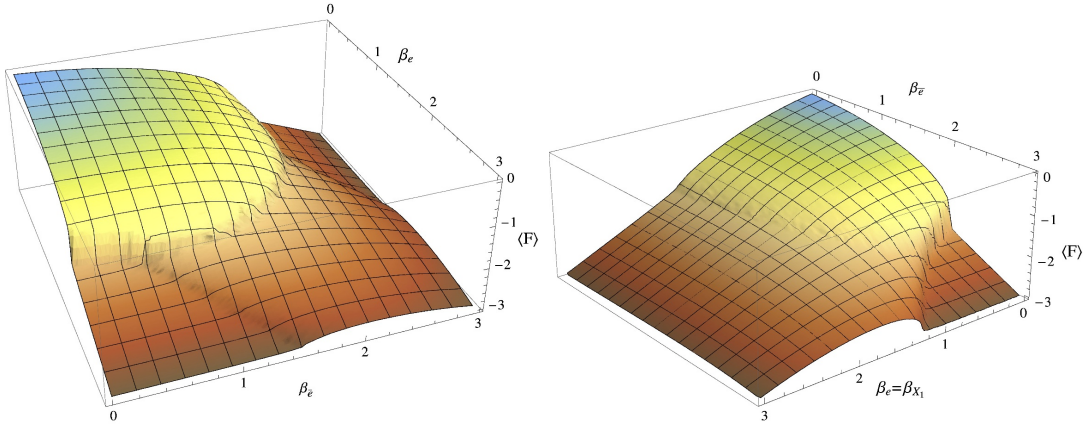


Figure 7. Plots of the free energy F for two-dimensional planes through the origin of the parameter space of the lattice model. In the left figure we have the $(\beta_e, \beta_{\bar{e}})$ plane and in the right figure we have the $(\beta_e = \beta_{X_1}, \beta_{\bar{e}})$ plane. See text for further comments.

all other couplings equal zero. For small values of all the couplings appearing in the action (34), we are in the completely confining phase of the gauge theory, where all the open string operators of magnetic flux have a non-zero expectation value, and all loop operators carrying electric charge are confined. This corresponds to the plateau in the graph where F is maximal and tends to zero.

The regions where the magnetic flux $(\bar{e}, 1)$ and (X_1, Γ^0) have condensed can be anticipated on theoretical grounds by realizing that the coupling β_A is inversely proportional to the mass of flux A . In fact, when we look at the subgroup K_A generated by the elements in class A , in particular

$$\begin{aligned} K_{\bar{e}} &= \{\mathbf{1}, -\mathbf{1}\} \\ K_{X_1} &= \{\mathbf{1}, -\mathbf{1}, i\sigma_1, -i\sigma_1\}, \end{aligned}$$

and set the couplings for the classes containing the elements in K_A equal to one another,

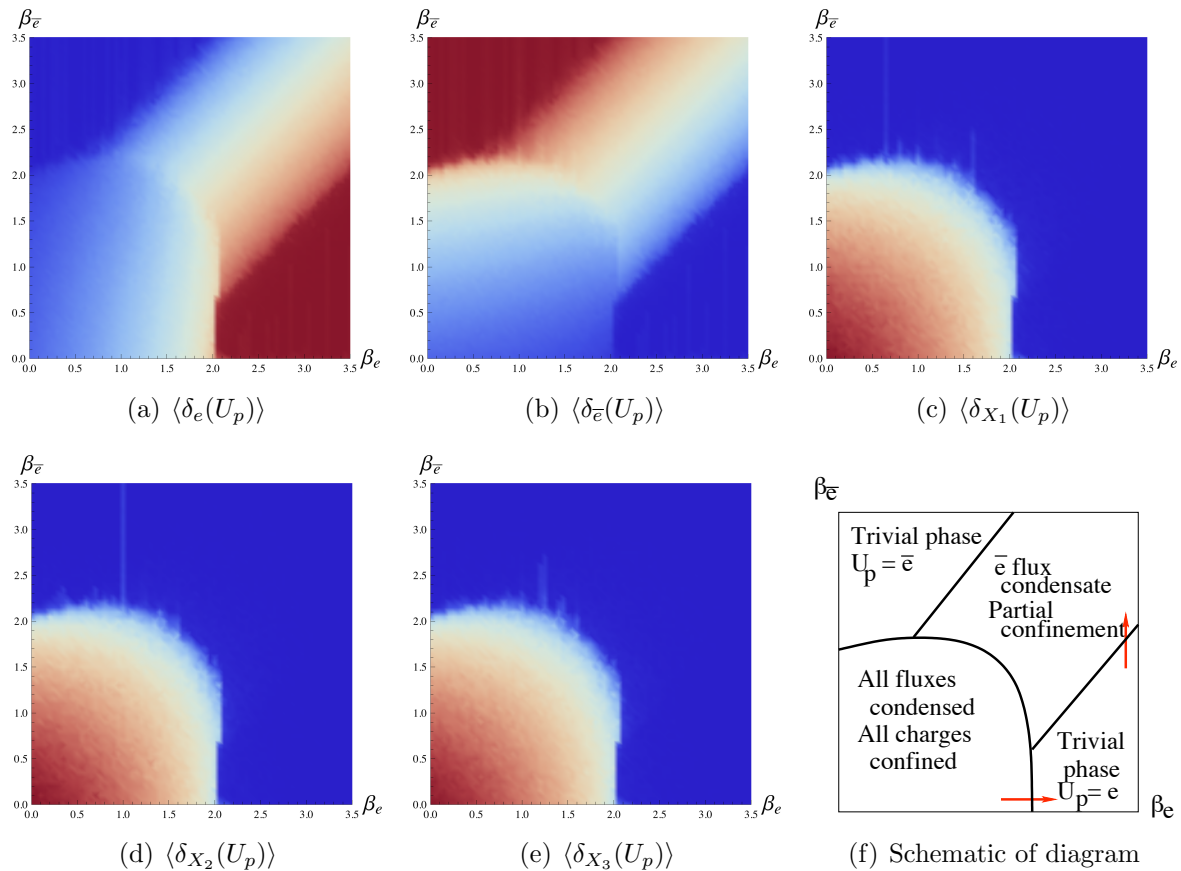


Figure 8. Space-time averaged expectation value of $\delta_A(U_p)$ for each class A . Shown is a $(\beta_e, \beta_{\bar{e}})$ -plane in coupling constant space where the other three couplings are zero. The color coding is such that red is the highest and blue the lowest value in each figure. In (f) we have identified the meaning of the various regions and the transition lines, where the red arrows indicate the trajectories used to determine whether the transitions are first or second order (see figure 11f and 12f).

there is an extra gauge invariance $U_p \rightarrow k U_p$ for an element $k \in A$ in the plaquette action (34). In particular

$$S = \beta (\delta_e(U_p) + \delta_{\bar{e}}(U_p))$$

is invariant with respect to $U_p \rightarrow -1 U_p$ and

$$S = \beta (\delta_e(U_p) + \delta_{\bar{e}}(U_p) + \delta_{X_1}(U_p))$$

is invariant with respect to $U_p \rightarrow k U_p$, where $k \in \{-1, i\sigma_1, -i\sigma_1\}$.

These left multiplications are exactly the kind appearing in the definition of the (loop) order parameters (28). Therefore one can establish, even without reverting to MC measurements, that the above actions, for large values of β , produce the desired flux condensates.

One may verify this reasoning in the Figures 8 and 9 where we have probed the phase diagram more in detail by measuring the spacetime averaged expectation value of $\delta_A(U_p)$ for all classes A as a function of the relevant coupling parameters β . The red

color indicates high values for the expectation value and we see that for all coupling parameters near zero all fluxes are condensed and thus all charges will be confined. This is what traditionally is called the “strong coupling phase ($g \sim 1/\beta \gg 1$). Looking at the colorings for the various operators one readily identifies the various phases as indicated in the schematics of the subfigures (f). For example the symmetry with respect to the diagonal of the Figures 8a and 8b, shows that there are “Ising” like ordered phases, one with all plaquette values $U_p = e$ and the other with all $U_p = \bar{e}$. The in-between region is the region with the \bar{e} flux condensate.

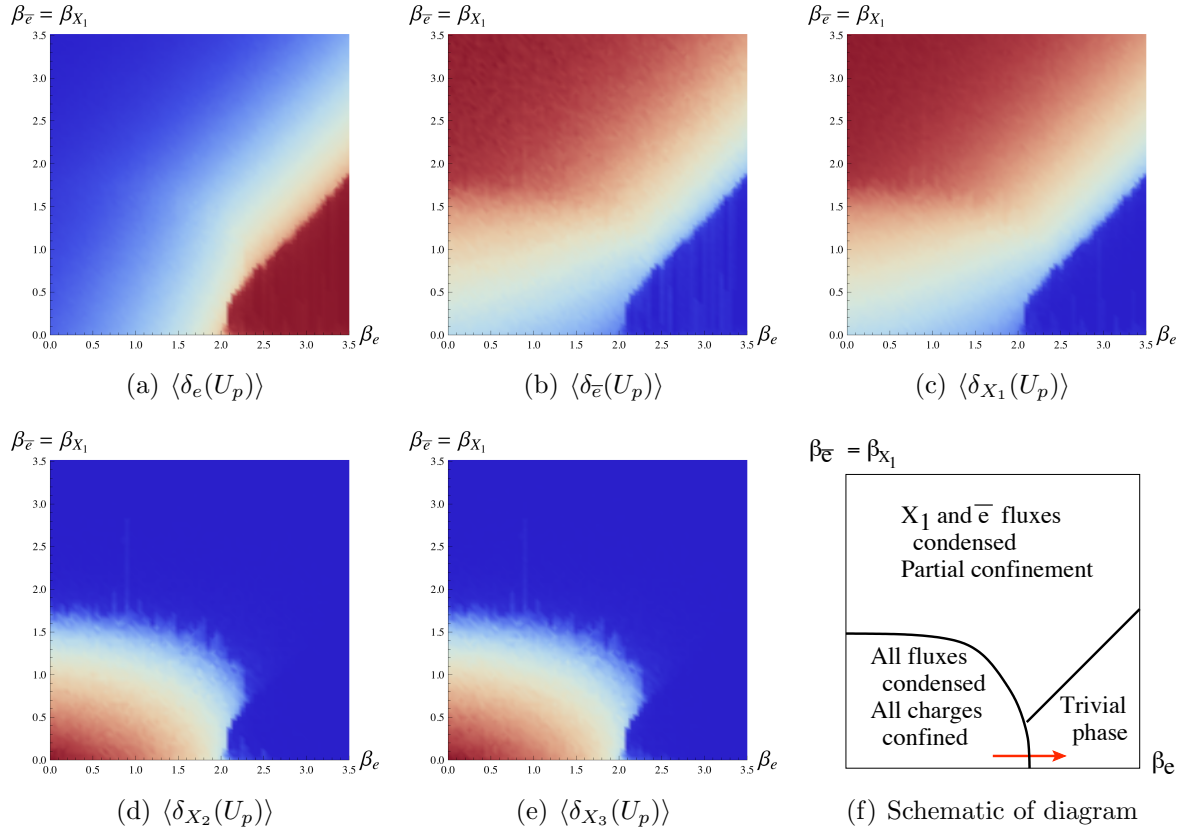


Figure 9. Space-time averaged expectation value of $\delta_A(U_p)$ for each class A . Shown is a $(\beta_e, \beta_{\bar{e}} = \beta_{X_1})$ -plane in coupling constant space where the other two couplings are zero. The color coding is such that red is the highest and blue the lowest value in each figure. In (f) we have identified the meaning of the various regions and the transition lines, where the red arrow indicates the trajectory used to determine whether the transition is first or second order (see figure 11f).

In the region with β_e larger than approximately 2.0 and all other couplings near zero, the trivial vacuum is realized. All string operators with nontrivial magnetic flux have zero expectation value there.

As pointed out in previous sections for example in relation (11), there is a very direct way to determine the condensate as well as the quantum embedding index q . This is by measuring the expectation value of the open string for each pure flux A and

then summing over all fluxes. In the $(\bar{e}, 1)$ vacuum we obtain

$$\left\langle \left| \uparrow_{(e,1)} \right\rangle_{\Phi} = \left\langle \left| \uparrow_{(\bar{e},1)} \right\rangle_{\Phi} = 1.0,$$

so $q = 2$, whereas in the (X_1, Γ^0) vacuum

$$\left\langle \left| \uparrow_{(e,1)} \right\rangle_{\Phi} = \left\langle \left| \uparrow_{(\bar{e},1)} \right\rangle_{\Phi} = 1.0, \quad \left\langle \left| \uparrow_{(X_1, \Gamma^0)} \right\rangle_{\Phi} = 2.0,$$

so in this case $q = 4$. In Figure 10 we show the measurement of the vacuum expectation value for the $(\bar{e}, 1)$ open string as a function of the coupling constant $\beta_{\bar{e}}$, which demonstrates that such measurements clearly indicate where the transition takes place.

There is one more issue we like to address in our simulations, that is to determine the order of the transitions we have identified. A conventional approach is to search for a hysteresis effect across a first order transition, but because of the relative modest size of the lattices used this is not an optimal approach. A method that is working much better is to directly probe the system at a given sequence of coupling constants around the transition and to see whether there is a coexistence region where both phases occur in the sampling \S . To perform these measurements we use the parallel tempering method [22] to overcome local minima in the action landscape. The idea behind this method is to initialize a range of lattices simultaneously, all at different couplings along a trajectory in coupling constant space starting in phase one and ending in phase two. The updates of this ensemble then consist of the updates of each of the individual lattices and, occasionally, a swap of two adjacent lattices. The swap between lattices **1** and **2** is accepted with a probability

$$p(\mathbf{1} \leftrightarrow \mathbf{2}) = \min \left\{ 1, \frac{\exp(S_1(\mathbf{1}) + S_2(\mathbf{2}))}{\exp(S_2(\mathbf{1}) + S_1(\mathbf{2}))} \right\},$$

where $S_1(\mathbf{2})$ means using the action (in particular, the set of couplings) of lattice **1** to evaluate the field configuration of lattice **2** et cetera. One can prove that this satisfies detailed balance. In effect, each lattice will perform a random walk through coupling constant space along the chosen trajectory, allowing a ‘‘cold’’ lattice to thermalize in the ‘‘high temperature’’ region, thus overcoming the local minima of the action.

We have made measurements for the trajectories indicated by the arrows in the Figures 8f and 9f. The results of these measurements for the horizontal arrow is given in Figure 11 and for the vertical arrow in Figure 12. We find that in that the horizontal trajectory the transition from the strongly coupled phase corresponding to the left peak in Figure 11 to the trivial phase corresponding to the right peak indeed goes through a coexistence region corresponding to the values of the coupling parameter where both peaks are present as in subfigures 11b and 11c. The result for the vertical trajectory corresponding to the transition from the trivial phase to the broken (X_1, Γ_0) phase is given in figure 12, where we see that the peak shifts continuously implying that the transition is second order.

\S We would like to thank Simon Trebst for pointing this out to us.

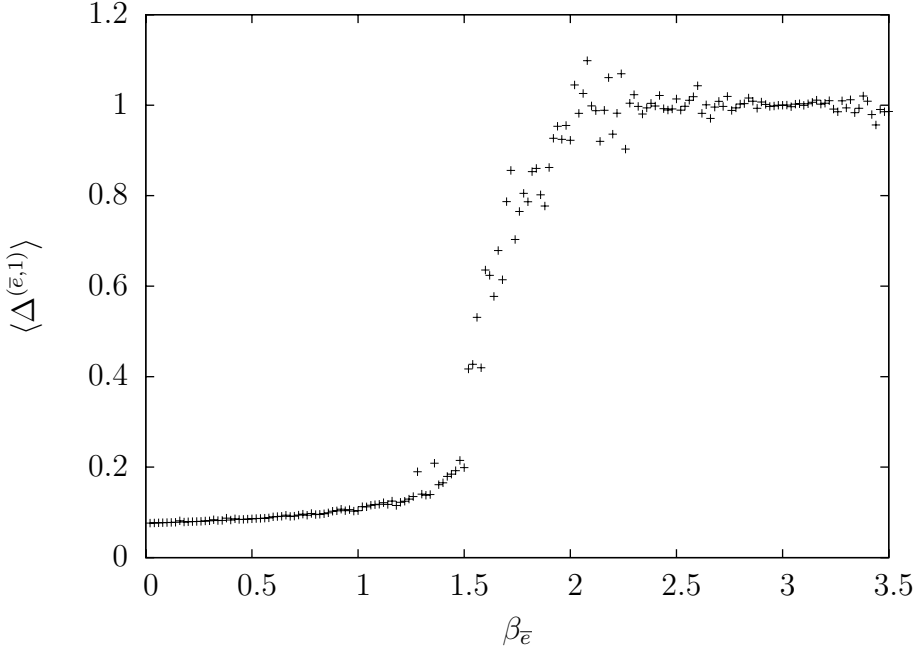


Figure 10. Vacuum expectation value of the $(\bar{e}, 1)$ open string as a function of the coupling constant $\beta_{\bar{e}}$, showing that the nonlocal open string operators are good order parameters to characterize topological phase transitions. Length of the string: 4 plaquettes, measurements on a 16^3 lattice, $\beta_e = 3.0$, other couplings zero.

Measuring the (broken) modular S -matrices. We have measured the (broken) S -matrix elements using the simple algorithm involving the auxiliary symmetries of our loop operators. This allows us to obtain the unbroken S -matrix as well as the branching matrix $n_u^{a_1}$ and the S -matrix of the effective \mathcal{U} theory in the various broken phases. Here we exploit the relation (22) for the measurement, and relation (17) :

$$S_{uv} = \frac{1}{q} \sum_{a_i, b_j} n_u^{a_i} n_v^{b_j} \langle S_{a_i b_j} \rangle_{\Phi},$$

relating S_{uv} to the measured S -matrix in the broken phase. We first measured the unbroken S -matrix in the $D(\bar{D}_2)$ phase and obtain results identical to the matrix calculated using defining formula (5), the result is given in Table 2 and is of course also consistent to the matrix obtained from the relation (17) with $\Phi = 0$. The accuracy of the measured matrix elements in represented in the table as integers is smaller than 5%.

The branching matrices n_u^a can be obtained from measuring the broken S -matrices. The columns in these matrices correspond to the different \mathcal{U} sectors. If we see two rows or columns with different parents a, b in the \mathcal{A} theory that are proportional to each other, a and b branch to the same \mathcal{U} sector u . Conversely, if different u fields correspond to the same a field that means that the a splits in the broken phase. We have listed the results for the broken S -matrix in the $(\bar{e}, 1)$ vacuum in Table 3.

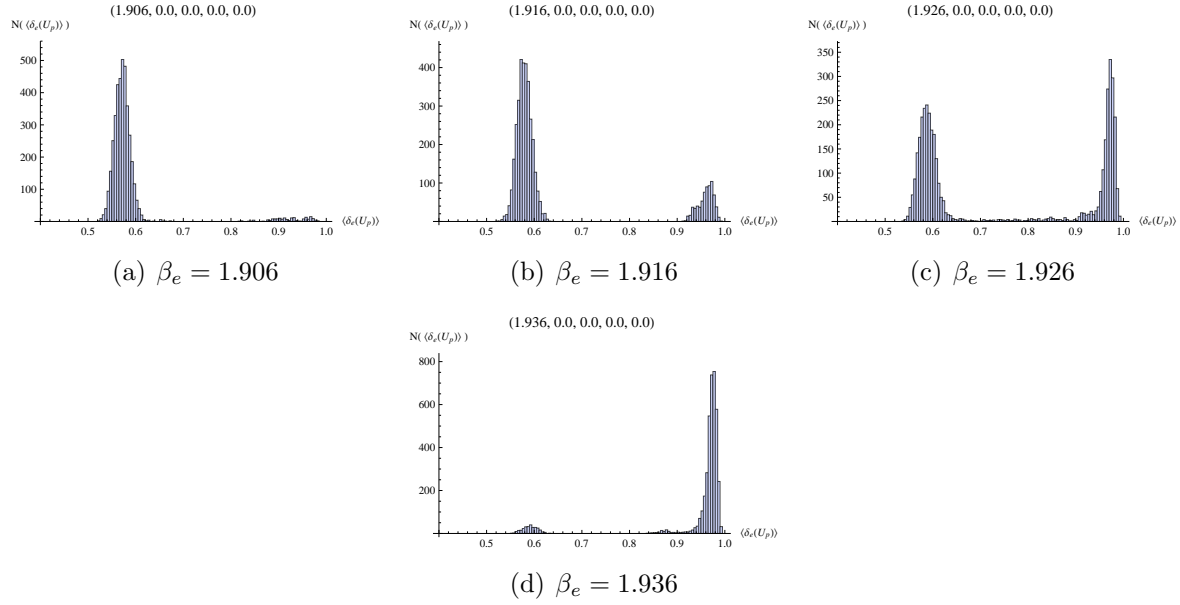


Figure 11. The sequence of plots is across the transition from the strongly coupled phase with all fluxes condensed and all charges confined, to the trivial phase. This trajectory corresponds to the horizontal arrow in figures 8f and 9f, where $1.906 \leq \beta_e \leq 1.936$ and all other couplings equal zero. Plotted along the x -axis is average expectation value of the percentage of trivial plaquettes with $U_p = e$ and along the y -axis we plot the number of times that that percentage is measured in a simulation of 4000 runs on a 10^3 lattice. The figures clearly show a shift from peak on the left to on the right, with a double peak in between, this is the signature of region where both phases coexist, i.e. of a first order transition.

	$(e, 1)$	(e, J_1)	(e, J_2)	(e, J_3)	(e, χ)	$(\bar{e}, 1)$	(\bar{e}, J_1)	(\bar{e}, J_2)	(\bar{e}, J_3)	(\bar{e}, χ)	(X_1, Γ^0)	(X_1, Γ^1)	(X_1, Γ^2)	(X_1, Γ^3)	(X_2, Γ^0)	(X_2, Γ^1)	(X_2, Γ^2)	(X_2, Γ^3)	(X_3, Γ^0)	(X_3, Γ^1)	(X_3, Γ^2)	(X_3, Γ^3)
$(e, 1)$	1	1	1	1	2	1	1	1	1	2	2	2	2	2	2	2	2	2	2	2	2	2
(e, J_1)	1	1	1	1	2	1	1	1	1	2	2	2	2	2	-2	-2	-2	-2	-2	-2	-2	-2
(e, J_2)	1	1	1	1	2	1	1	1	1	2	-2	-2	-2	-2	2	2	2	2	-2	-2	-2	-2
(e, J_3)	1	1	1	1	2	1	1	1	1	2	-2	-2	-2	-2	-2	-2	-2	-2	2	2	2	2
(e, χ)	2	2	2	2	4	-2	-2	-2	-2	-4	0	0	0	0	0	0	0	0	0	0	0	0
$(\bar{e}, 1)$	1	1	1	1	-2	1	1	1	1	-2	2	2	2	2	2	2	2	2	2	2	2	2
(\bar{e}, J_1)	1	1	1	1	-2	1	1	1	1	-2	2	2	2	2	-2	-2	-2	-2	-2	-2	-2	-2
(\bar{e}, J_2)	1	1	1	1	-2	1	1	1	1	-2	-2	-2	-2	-2	2	2	2	2	-2	-2	-2	-2
(\bar{e}, J_3)	1	1	1	1	-2	1	1	1	1	-2	-2	-2	-2	-2	-2	-2	-2	-2	2	2	2	2
(\bar{e}, χ)	2	2	2	2	-4	-2	-2	-2	-2	4	0	0	0	0	0	0	0	0	0	0	0	0
(X_1, Γ^0)	2	2	-2	-2	0	2	2	-2	-2	0	4	0	0	-4	0	0	0	0	0	0	0	0
(X_1, Γ^1)	2	2	-2	-2	0	2	2	-2	-2	0	0	-4	0	4	0	0	0	0	0	0	0	0
(X_1, Γ^2)	2	2	-2	-2	0	2	2	-2	-2	0	-4	0	4	0	0	0	0	0	0	0	0	0
(X_1, Γ^3)	2	2	-2	-2	0	2	2	-2	-2	0	0	4	0	-4	0	0	0	0	0	0	0	0
(X_2, Γ^0)	2	-2	2	-2	0	2	-2	2	-2	0	0	0	0	0	4	0	-4	0	0	0	0	0
(X_2, Γ^1)	2	-2	2	-2	0	2	-2	2	-2	0	0	0	0	0	0	-4	0	4	0	0	0	0
(X_2, Γ^2)	2	-2	2	-2	0	2	-2	2	-2	0	0	0	0	0	-4	0	4	0	0	0	0	0
(X_2, Γ^3)	2	-2	2	-2	0	2	-2	2	-2	0	0	0	0	0	0	4	0	-4	0	0	0	0
(X_3, Γ^0)	2	-2	-2	2	0	2	-2	-2	2	0	0	0	0	0	0	0	0	0	4	0	-4	0
(X_3, Γ^1)	2	-2	-2	2	0	2	-2	-2	2	0	0	0	0	0	0	0	0	0	0	-4	0	4
(X_3, Γ^2)	2	-2	-2	2	0	2	-2	-2	2	0	0	0	0	0	0	0	0	0	-4	0	4	0
(X_3, Γ^3)	2	-2	-2	2	0	2	-2	-2	2	0	0	0	0	0	0	0	0	0	4	0	0	-4

Table 2. The S -matrix for the (unbroken) $D(\bar{D}_2)$ theory (up to the normalisation factor $1/D_A = 1/8$) as measured in the trivial vacuum. We put integers in the table as the accuracy is below the 5%, i.e. 1 actually stands for read as $1. \pm 0.05$.

To realize the splittings between the irreducible representations using the auxiliary gauge symmetries alluded to in section 2.2, we found the following construction to suffice.

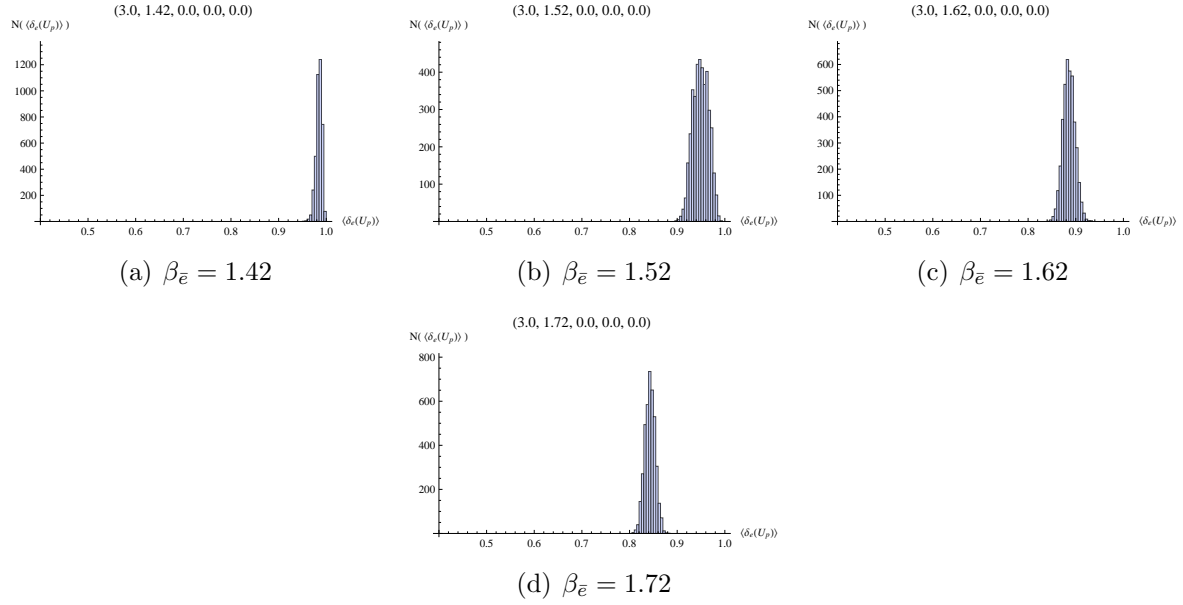


Figure 12. The sequence of plots is across the transition from the trivial phase to the phase with the \bar{e} condensate, the trajectory corresponds to the vertical arrow in figure 8f, where $1.42 \leq \beta_{\bar{e}} \leq 1.72$, $\beta_e = 3.0$ and all other couplings equal zero. Plotted along the x-axis is average expectation value of the percentage of trivalent plaquettes with $U_p = e$ and along the y-axis we plot the number of times that that percentage is measured in a simulation of 4000 runs on a 10^3 lattice. The figures only feature only a single peak that smoothly moves from one phase to the other, indicating a smooth second order transition.

$(\bar{e}, 1)$ vacuum

- $(X_i, \Gamma^0)_1$ is realized by the operator $\Delta^{(X_i, \Gamma^0)}$.
- $(X_i, \Gamma^0)_2$ is realized by the operators $\Delta^{(X_i, \Gamma^0)} \Delta^{(e, J_i)}$.
- $(X_1, \Gamma^2)_1$ is realized by the operator $\Delta^{(X_1, \Gamma^2)}$ with $\{x_{i\sigma_1} = e, x_{-i\sigma_1} = i\sigma_2\}$.
- $(X_1, \Gamma^2)_2$ is realized by the operators $\Delta^{(X_1, \Gamma^2)} \Delta^{(e, J_1)}$ with $\{x_{i\sigma_1} = e, x_{-i\sigma_1} = i\sigma_2\}$.
- $(X_2, \Gamma^2)_1$ is realized by the operator $\Delta^{(X_2, \Gamma^2)}$ with $\{x_{i\sigma_2} = e, x_{-i\sigma_2} = i\sigma_1\}$.
- $(X_2, \Gamma^2)_2$ is realized by the operators $\Delta^{(X_2, \Gamma^2)} \Delta^{(e, J_2)}$ with $\{x_{i\sigma_2} = e, x_{-i\sigma_2} = i\sigma_1\}$.
- $(X_3, \Gamma^2)_1$ is realized by the operator $\Delta^{(X_3, \Gamma^2)}$ with $\{x_{i\sigma_3} = e, x_{-i\sigma_3} = i\sigma_1\}$.
- $(X_3, \Gamma^2)_2$ is realized by the operators $\Delta^{(X_3, \Gamma^2)} \Delta^{(e, J_3)}$ with $\{x_{i\sigma_3} = e, x_{-i\sigma_3} = i\sigma_1\}$.

(X_1, Γ^0) vacuum

- $(X_i, \Gamma^0)_1$ is realized by the operator $\Delta^{(X_i, \Gamma^0)}$.
- $(X_1, \Gamma^0)_2$ is realized by the operators $\Delta^{(X_1, \Gamma^0)} \Delta^{(e, J_1)}$.
- $(X_2, \Gamma^2)_1$ is realized by the operator $\Delta^{(X_2, \Gamma^2)}$ with $\{x_{i\sigma_2} = e, x_{-i\sigma_2} = i\sigma_1\}$.
- $(X_3, \Gamma^2)_1$ is realized by the operator $\Delta^{(X_3, \Gamma^2)}$ with $\{x_{i\sigma_3} = e, x_{-i\sigma_3} = i\sigma_1\}$.

We see that in Table 3 the columns (rows) for the sectors (e, α) and (\bar{e}, α) for $\alpha = 1, J_1, J_2, J_3$ are identical and thus that the corresponding fields have to be identified. This leaves us with 16 sectors for the broken \mathcal{U} theory. Summing the entries as prescribed

	$(e, 1)$	(e, J_1)	(e, J_2)	(e, J_3)	$(\bar{e}, 1)$	(\bar{e}, J_1)	(\bar{e}, J_2)	(\bar{e}, J_3)	$(X_1, \Gamma^0)_1$	$(X_1, \Gamma^0)_2$	$(X_1, \Gamma^2)_1$	$(X_1, \Gamma^2)_2$	$(X_2, \Gamma^0)_1$	$(X_2, \Gamma^0)_2$	$(X_2, \Gamma^2)_1$	$(X_2, \Gamma^2)_2$	$(X_3, \Gamma^0)_1$	$(X_3, \Gamma^0)_2$	$(X_3, \Gamma^2)_1$	$(X_3, \Gamma^2)_2$
$(e, 1)$	1	1	1	1	1	1	1	1	2	2	2	2	2	2	2	2	2	2	2	2
(e, J_1)	1	1	1	1	1	1	1	1	2	2	2	2	-2	-2	-2	-2	-2	-2	-2	-2
(e, J_2)	1	1	1	1	1	1	1	1	-2	-2	-2	-2	2	2	2	2	2	2	2	2
(e, J_3)	1	1	1	1	1	1	1	1	-2	-2	-2	-2	2	2	2	2	2	2	2	2
$(\bar{e}, 1)$	1	1	1	1	1	1	1	1	2	2	2	2	2	2	2	2	2	2	2	2
(\bar{e}, J_1)	1	1	1	1	1	1	1	1	2	2	2	2	-2	-2	-2	-2	-2	-2	-2	-2
(\bar{e}, J_2)	1	1	1	1	1	1	1	1	-2	-2	-2	-2	2	2	2	2	2	2	2	2
(\bar{e}, J_3)	1	1	1	1	1	1	1	1	-2	-2	-2	-2	2	2	2	2	2	2	2	2
$(X_1, \Gamma^0)_1$	2	2	-2	-2	2	2	-2	-2	4	4	-4	-4	4	4	-4	-4	4	4	-4	-4
$(X_1, \Gamma^0)_2$	2	2	-2	-2	2	2	-2	-2	4	4	-4	-4	4	4	-4	-4	4	4	-4	-4
$(X_1, \Gamma^2)_1$	2	2	-2	-2	2	2	-2	-2	-4	-4	4	4	-4	-4	4	4	-4	-4	4	4
$(X_1, \Gamma^2)_2$	2	2	-2	-2	2	2	-2	-2	-4	-4	4	4	-4	-4	4	4	-4	-4	4	4
$(X_2, \Gamma^0)_1$	2	-2	2	-2	2	-2	2	-2	4	4	-4	-4	4	4	-4	-4	4	4	-4	-4
$(X_2, \Gamma^0)_2$	2	-2	2	-2	2	-2	2	-2	-4	-4	4	4	-4	-4	4	4	-4	-4	4	4
$(X_2, \Gamma^2)_1$	2	-2	2	-2	2	-2	2	-2	4	4	-4	-4	4	4	-4	-4	4	4	-4	-4
$(X_2, \Gamma^2)_2$	2	-2	2	-2	2	-2	2	-2	-4	-4	4	4	-4	-4	4	4	-4	-4	4	4
$(X_3, \Gamma^0)_1$	2	-2	-2	2	2	-2	-2	2	4	4	-4	-4	4	4	-4	-4	4	4	-4	-4
$(X_3, \Gamma^0)_2$	2	-2	-2	2	2	-2	-2	2	-4	-4	4	4	-4	-4	4	4	-4	-4	4	4
$(X_3, \Gamma^2)_1$	2	-2	-2	2	2	-2	-2	2	4	4	-4	-4	4	4	-4	-4	4	4	-4	-4
$(X_3, \Gamma^2)_2$	2	-2	-2	2	2	-2	-2	2	-4	-4	4	4	-4	-4	4	4	-4	-4	4	4

Table 3. The broken S -matrix as measured in the $(\bar{e}, 1)$ vacuum, where the columns and rows of zeroes corresponding to the confined fields are left out. Identifying identical columns and rows we obtain the familiar S -matrix of the $D(\mathbb{Z}_2 \otimes \mathbb{Z}_2)$ theory.

\mathcal{U}	$D(\mathbb{Z}_2 \otimes \mathbb{Z}_2)$	$(e, 1)$	(e, J_1)	(e, J_2)	(e, J_3)	$(X_1, \Gamma^0)_1$	$(X_1, \Gamma^0)_2$	$(X_1, \Gamma^2)_1$	$(X_1, \Gamma^2)_2$	$(X_2, \Gamma^0)_1$	$(X_2, \Gamma^0)_2$	$(X_2, \Gamma^2)_1$	$(X_2, \Gamma^2)_2$	$(X_3, \Gamma^0)_1$	$(X_3, \Gamma^0)_2$	$(X_3, \Gamma^2)_1$	$(X_3, \Gamma^2)_2$
		$(e, 1)$	$(+, +, +)$	1	1	1	1	1	1	1	1	1	1	1	1	1	1
(e, J_1)	$(+, +, -)$	1	1	1	1	1	1	1	1	-1	-1	-1	-1	-1	-1	-1	-1
(e, J_2)	$(+, +, -)$	1	1	1	1	-1	-1	-1	-1	1	1	1	1	-1	-1	-1	-1
(e, J_3)	$(+, +, -)$	1	1	1	1	-1	-1	-1	-1	-1	-1	-1	-1	1	1	1	1
$(X_1, \Gamma^0)_1$	$(+, +, +)$	1	1	-1	-1	1	1	-1	-1	1	-1	1	-1	1	-1	1	-1
$(X_1, \Gamma^0)_2$	$(+, +, +)$	1	1	-1	-1	1	1	-1	-1	-1	-1	-1	-1	1	-1	1	-1
$(X_1, \Gamma^2)_1$	$(+, +, -)$	1	1	-1	-1	-1	-1	1	1	1	-1	1	-1	-1	1	-1	1
$(X_1, \Gamma^2)_2$	$(+, +, -)$	1	1	-1	-1	-1	-1	1	1	-1	1	-1	1	-1	1	-1	1
$(X_2, \Gamma^0)_1$	$(+, +, +)$	1	-1	1	-1	1	1	-1	1	1	-1	1	-1	1	-1	1	-1
$(X_2, \Gamma^0)_2$	$(+, +, +)$	1	-1	1	-1	-1	1	-1	1	1	-1	-1	-1	-1	1	1	-1
$(X_2, \Gamma^2)_1$	$(+, +, -)$	1	-1	1	-1	1	1	-1	-1	-1	1	1	-1	1	-1	1	-1
$(X_2, \Gamma^2)_2$	$(+, +, -)$	1	-1	1	-1	-1	1	-1	1	-1	1	1	-1	-1	1	-1	1
$(X_3, \Gamma^0)_1$	$(-, -, +)$	1	-1	-1	1	1	-1	-1	1	1	-1	-1	1	1	-1	-1	1
$(X_3, \Gamma^0)_2$	$(-, -, +)$	1	-1	-1	1	-1	1	-1	-1	1	1	-1	-1	1	-1	-1	1
$(X_3, \Gamma^2)_1$	$(-, -, -)$	1	-1	-1	1	1	-1	-1	1	-1	1	-1	-1	1	-1	-1	1
$(X_3, \Gamma^2)_2$	$(-, -, -)$	1	-1	-1	1	-1	1	-1	-1	-1	-1	1	-1	-1	1	-1	1

Table 4. The S -matrix of the $\mathcal{U} = D(\mathbb{Z}_2 \otimes \mathbb{Z}_2)$ theory (up to normalisation factor of $1/D_U = 1/4$) as obtained from the broken S -matrix measured in the $(\bar{e}, 1)$ vacuum, after leaving out the rows and columns with only zeroes of the confined fields and after identifying identical rows and columns.

by formula (3.3) yields exactly the S -matrix of the $D(\mathbb{Z}_2 \otimes \mathbb{Z}_2)$ theory, which is given in Table 4.

In Table 5 we have listed the result for broken S -matrix in the (X_1, Γ^0) vacuum. here we have to identify the sectors $(e, 1)$, $(\bar{e}, 1)$ and $(X_1, \Gamma^0)_1$, the sectors (e, J_1) , (\bar{e}, J_1) and $(X_1, \Gamma^0)_2$, the sectors $(X_2, \Gamma^0)_1$ and $(X_3, \Gamma^0)_1$, and the sectors $(X_2, \Gamma^2)_1$ and $(X_3, \Gamma^2)_1$. These results are all fully consistent with the algebraic analysis presented in Section 3.1.

Let us illustrate the method by calculating a few sample S -matrix elements in the (X_1, Γ^0) condensed vacuum. The \mathcal{U} theory should be $D(\mathbb{Z}_2)$; let us first calculate the $S_{(+, +)(+, +)}$ element, the $(+, +)$ sector being the new vacuum

$$S_{(+, +)(+, +)} = \frac{1}{q} \left\{ \langle S_{(e, 1)(e, 1)} \rangle_{\Phi} + \langle S_{(e, 1)(\bar{e}, 1)} \rangle_{\Phi} + \langle S_{(e, 1)(X_1, \Gamma^0)} \rangle_{\Phi} + \right.$$

	$(e, 1)$	(e, J_1)	$(\bar{e}, 1)$	(\bar{e}, J_1)	$(X_1, \Gamma^0)_1$	$(X_1, \Gamma^0)_2$	$(X_2, \Gamma^0)_1$	$(X_2, \Gamma^2)_1$	$(X_3, \Gamma^0)_1$	$(X_3, \Gamma^2)_1$
$(e, 1)$	1	1	1	1	2	2	2	2	2	2
(e, J_1)	1	1	1	1	2	2	-2	-2	-2	-2
$(\bar{e}, 1)$	1	1	1	1	2	2	2	2	2	2
(\bar{e}, J_1)	1	1	1	1	2	2	-2	-2	-2	-2
$(X_1, \Gamma^0)_1$	2	2	2	2	4	4	4	4	4	4
$(X_1, \Gamma^0)_2$	2	2	2	2	4	4	-4	-4	-4	-4
$(X_2, \Gamma^0)_1$	2	-2	2	-2	4	-4	4	-4	4	-4
$(X_2, \Gamma^2)_1$	2	-2	2	-2	4	-4	-4	4	-4	4
$(X_3, \Gamma^0)_1$	2	-2	2	-2	4	-4	4	-4	4	-4
$(X_3, \Gamma^2)_1$	2	-2	2	-2	4	-4	-4	4	-4	4

Table 5. The broken S -matrix for the $D(\bar{D}_2)$ theory as measured in the (X_1, Γ^0) vacuum.

$$\begin{aligned}
 & \langle S_{(\bar{e},1)(e,1)} \rangle_{\Phi} + \langle S_{(\bar{e},1)(\bar{e},1)} \rangle_{\Phi} + \langle S_{(\bar{e},1)(X_1, \Gamma^0)} \rangle_{\Phi} + \\
 & \langle S_{(X_1, \Gamma^0)(e,1)} \rangle_{\Phi} + \langle S_{(X_1, \Gamma^0)(\bar{e},1)} \rangle_{\Phi} + \langle S_{(X_1, \Gamma^0)(X_1, \Gamma^0)} \rangle_{\Phi} \Big\} = \\
 & \frac{1}{4} \frac{1}{8} (1 + 1 + 2 + 1 + 1 + 2 + 2 + 2 + 4) = \frac{1}{2},
 \end{aligned}$$

in agreement with Table 6. The contributions to the above matrix element would be equal if we had used the S -matrix elements as measured in the trivial vacuum.

\mathcal{U}	$D(\mathbb{Z}_2)$	$(e, 1)$	(e, J_1)	$(X_2, \Gamma^0)_1$	$(X_2, \Gamma^2)_1$
$(e, 1)$	$(+, +)$	1	1	1	1
(e, J_1)	$(+, -)$	1	1	-1	-1
$(X_2, \Gamma^0)_1$	$(-, +)$	1	-1	1	-1
$(X_2, \Gamma^2)_1$	$(-, -)$	1	-1	-1	1

Table 6. The modular S -matrix for the $D(\mathbb{Z}_2)$ theory (up to normalisation factor $1/D_U = 1/2$)

To appreciate the importance of the measurements in the broken vacuum, consider the matrix element $S_{(-,+)(-,-)}$. The parents of the $(-, +)$ sector are $(X_2, \Gamma^0)_1$ and $(X_3, \Gamma^0)_1$ and those of the $(-, -)$ are $(X_2, \Gamma^2)_1$ and $(X_3, \Gamma^2)_1$.

$$\begin{aligned}
 S_{(-,+)(-,-)} &= \frac{1}{q} \left\{ \langle S_{(X_2, \Gamma^0)_1(X_2, \Gamma^2)_1} \rangle_{\Phi} + \langle S_{(X_2, \Gamma^0)_1(X_3, \Gamma^2)_1} \rangle_{\Phi} + \right. \\
 & \left. \langle S_{(X_3, \Gamma^0)_1(X_2, \Gamma^2)_1} \rangle_{\Phi} + \langle S_{(X_3, \Gamma^0)_1(X_3, \Gamma^2)_1} \rangle_{\Phi} \right\} = \\
 & \frac{1}{4} \frac{1}{8} ((-4) + (-4) + (-4) + (-4)) = -\frac{1}{2},
 \end{aligned}$$

. We see that after completing the calculation along this line we obtain the S -matrix of the $D(\mathbb{Z})$ theory, as given in Table 6. Note that if we had used the S -matrix of the unbroken theory, the $S_{(X_2, \Gamma^0)(X_3, \Gamma^2)}$ and $S_{(X_3, \Gamma^0)(X_2, \Gamma^2)}$ would have been zero.

4. Conclusions and outlook

In this article we have studied euclidean lattice models for Discrete Gauge Theories. We have introduced a set of multiparameter actions for these theories that display a rich phase structure, and showed in particular that all the allowed condensates of pure

magnetic flux are realized in certain well anticipated regions of coupling constant space. The set of open string operators that we defined form a set of order parameters that allowed us to determine the content of the condensate and to measure the topological symmetry breaking index q .

Furthermore, we have shown that it is possible to unambiguously reconstruct the S -matrix of the low-energy theory in a broken or unbroken phase by measurements of the braided loop operators we did propose in earlier work [20]. Due to an auxiliary gauge symmetry these operators are particularly well suited to detect the nontrivial splittings of fields that correspond to fixed points under fusion with the condensate. We found that as expected the excitations that are confined in a broken vacuum give rise to rows and columns of zeroes in the broken S -matrix. Our work clearly demonstrates that the euclidean approach allows for a very straightforward method to completely determine the nature of the broken phase.

Our work showed that the reason the modular S -matrix changes in the broken phase is largely due to the contribution of the so-called vacuum exchange diagram. In an upcoming more theoretical paper [12] we will extend the approach used in this work, the use of observables and in particular the S -matrix to determine the phase structure of a TQFT to a far wider range of theories, in particular the $SU(N)_k$ TQFT arising from Chern-Simons actions.

It would be interesting to study different models exhibiting different topological phases by somehow formulating them in the euclidean 3-dimensional framework, to our knowledge such an approach is unfortunately not yet available for Chern Simons theories. One expects that for Levin Wen models [23] our approach could be implemented though.

The authors would like to thank Jan Smit, Joost Slingerland, Simon Trebst and Sebas Eliëns for useful discussions. JCR is financially supported by a grant from FOM.

Appendix A. Fusion rules for \bar{D}_2 DGT

$$\begin{aligned}
(e, J_i) \times (e, J_i) &= (e, 1) \\
(e, J_i) \times (e, J_j) &= (e, J_k) \\
(e, J_i) \times (e, \chi) &= (e, \chi) \\
(e, \chi) \times (e, \chi) &= (e, 1) + \sum (e, J_i) \\
(\bar{e}, 1) \times (e, J_i) &= (\bar{e}, J_i) \\
(\bar{e}, 1) \times (e, \chi) &= (\bar{e}, \chi) \\
(e, J_i) \times (X_i, \Gamma^{0,2}) &= (X_i, \Gamma^{0,2}) \\
(e, J_i) \times (X_j, \Gamma^{0,2}) &= (X_j, \Gamma^{2,0}) \\
(e, \chi) \times (X_i, \Gamma^0) &= (X_i, \Gamma^1) + (X_i, \Gamma^3) \\
(\bar{e}, 1) \times (\bar{e}, 1) &= (e, 1) \\
(\bar{e}, 1) \times (X_i, \Gamma^{0,2}) &= (X_i, \Gamma^{0,2}) \\
(\bar{e}, 1) \times (X_i, \Gamma^{1,3}) &= (X_i, \Gamma^{3,1}) \\
(e, J_i) \times (X_i, \Gamma^{1,3}) &= (X_i, \Gamma^{1,3}) \\
(e, J_i) \times (X_j, \Gamma^{1,3}) &= (X_j, \Gamma^{3,1}) \\
(e, \chi) \times (X_i, \Gamma^{1,3}) &= (X_i, \Gamma^0) + (X_i, \Gamma^2) \\
(X_i, \Gamma^{0,2}) \times (X_i, \Gamma^{0,2}) &= (e, 1) + (\bar{e}, 1) + (e, J_i) + (\bar{e}, J_i) \\
(X_i, \Gamma^0) \times (X_i, \Gamma^2) &= (e, J_j) + (\bar{e}, J_j) + (e, J_k) + (\bar{e}, J_k) \\
(X_i, \Gamma^{0,2}) \times (X_j, \Gamma^{0,2}) &= (X_i, \Gamma^{2,0}) \times (X_j, \Gamma^{0,2}) = (X_k, \Gamma^0) + (X_k, \Gamma^2) \\
(X_i, \Gamma^{0,2}) \times (X_i, \Gamma^{1,3}) &= (X_i, \Gamma^{2,0}) \times (X_i, \Gamma^{1,3}) = (e, \chi) + (\bar{e}, \chi) \\
(X_i, \Gamma^{0,2}) \times (X_j, \Gamma^{1,3}) &= (X_i, \Gamma^{2,0}) \times (X_j, \Gamma^{1,3}) = (X_k, \Gamma^1) + (X_k, \Gamma^3) \\
(X_i, \Gamma^{1,3}) \times (X_i, \Gamma^{1,3}) &= (e, 1) + (e, J_i) + (\bar{e}, J_j) + (\bar{e}, J_k) \\
(X_i, \Gamma^1) \times (X_i, \Gamma^3) &= (\bar{e}, 1) + (\bar{e}, J_i) + (e, J_j) + (e, J_k) \\
(X_i, \Gamma^{1,3}) \times (X_j, \Gamma^{1,3}) &= (X_i, \Gamma^{3,1}) \times (X_j, \Gamma^{1,3}) = (X_k, \Gamma^0) + (X_k, \Gamma^2)
\end{aligned}$$

References

- [1] F. J. Burnell, S. H. Simon, and J. K. Slingerland. Phase transitions in topological lattice models via topological symmetry breaking. *ArXiv e-prints*, December 2010.
- [2] G. Kells, J. Kailasvuori, J. Slingerland, and J. Vala. Kaleidoscope of topological phases with multiple Majorana species. *ArXiv e-prints*, December 2010.
- [3] F.A. Bais, B.J. Schroers, and J.K. Slingerland. Broken quantum symmetry and confinement phases in planar physics. *Phys. Rev. Lett.*, 89:181601, 2002.
- [4] N. Read and D. Green. Paired states of fermions in two dimensions with breaking of parity and time-reversal symmetries and the fractional quantum Hall effect. *Phys. Rev. B*, 61:10267–10297, April 2000.
- [5] E. Grosfeld and K. Schoutens. Non-Abelian anyons: when Ising meets Fibonacci. arXiv: 0810.1955, 2008.
- [6] F. A. Bais, J. K. Slingerland, and S. M. Haaker. A theory of topological edges and domain walls. *Physical Review Letters*, 102:220403, 2009.
- [7] M. Barkeshli and X.-G. Wen. Bilayer quantum Hall phase transitions and the orbifold non-Abelian fractional quantum Hall states. *ArXiv e-prints*, October 2010.
- [8] M. Barkeshli and X.-G. Wen. Anyon Condensation and Continuous Topological Phase Transitions in Non-Abelian Fractional Quantum Hall States. *Physical Review Letters*, 105(21):216804–+, November 2010.
- [9] F.A. Bais and J.K. Slingerland. Condensate-induced transitions between topologically ordered

- phases. *Phys. Rev. B*, 79:045316, 2009.
- [10] Parsa Hassan Bonderson. Non-abelian anyons and interferometry. *Thesis (CalTech)*, 2007.
- [11] F. A. Bais and J. K. Slingerland. Topological entanglement entropy relations for multi phase systems with interfaces. *ArXiv e-prints*, June 2010.
- [12] F.A. Bais, S.Eliëns, and J. Romers. Topological symmetry breaking and tensor categories. (in preparation), 2011.
- [13] Erik P. Verlinde. Fusion Rules and Modular Transformations in 2D Conformal Field Theory. *Nucl. Phys.*, B300:360, 1988.
- [14] F.Alexander Bais, Peter van Driel, and Mark de Wild Propitius. Quantum symmetries in discrete gauge theories. *Phys.Lett.*, B280:63–70, 1992.
- [15] P. Roche, V. Pasquier, and R. Dijkgraaf. QuasiHopf algebras, group cohomology and orbifold models. *Nucl.Phys.Proc.Suppl.*, 18B:60–72, 1990.
- [16] Mark de Wild Propitius and F.Alexander Bais. Discrete gauge theories. 1995. Published in *Particles and Fields*. Edited by G.W. Semenoff. Berlin, Germany, Springer Verlag, 1998, (CRM Series in Math. Physics), pp. 353-440.
- [17] Kenneth G. Wilson. Confinement of Quarks. *Phys.Rev.*, D10:2445–2459, 1974.
- [18] A. Yu. Kitaev. Fault-tolerant quantum computation by anyons. *Annals of Physics*, 303(1):2 – 30, 2003.
- [19] John Kogut and Leonard Susskind. Hamiltonian formulation of wilson’s lattice gauge theories. *Phys. Rev. D*, 11(2):395–408, Jan 1975.
- [20] F.A. Bais and J.C. Romers. Anyonic order parameters for discrete gauge theories on the lattice. *Annals Phys.*, 324:1168–1175, 2009.
- [21] Mark G. Alford and John March-Russell. New order parameters for nonAbelian gauge theories. *Nucl.Phys.*, B369:276–298, 1992.
- [22] Koji Hukushima and Koji Nemoto. Exchange monte carlo method and application to spin glass simulations. *Journal of the Physical Society of Japan*, 65(6):1604–1608, 1996.
- [23] Michael Levin and Xiao-Gang Wen. Fermions, strings, and gauge fields in lattice spin models. *Phys.Rev.*, B67:245316, 2003.